

Citation for published version:

Ioanna D. Styliari, et al, 'High-Throughput Miniaturized Screening of Nanoparticle Formation via Inkjet Printing', *Macromolecular Materials and Engineering*, (2018).

DOI:

<https://doi.org/10.1002/mame.201800146>

Document Version:

This is the Accepted Manuscript version.

The version in the University of Hertfordshire Research Archive may differ from the final published version.

Copyright and Reuse:

© 2018 WILEY-VCH Verlag GmbH & Co. KGaA, Weinheim

This article may be used for non-commercial purposes in accordance with [Wiley Terms and Conditions for Self-Archiving](#).

Enquiries

If you believe this document infringes copyright, please contact Research & Scholarly Communications at rsc@herts.ac.uk

DOI: 10.1002/ ((please add manuscript number))

Article type: **Full Paper**

High throughput miniaturized screening of nanoparticle formation via inkjet printing

Ioanna D. Styliari, Claudia Conte, Amanda K. Pearce, Amanda Hüsler, Robert J. Cavanagh, Marion J. Limo, Dipak Gordhan, Alejandro Nieto-Orellana, Jiraphong Suksiriworapong, Benoit Couturaud, Phil Williams, Andrew L. Hook, Morgan R. Alexander, Martin C. Garnett, Cameron Alexander, Jonathan C. Burley* and Vincenzo Taresco**

Dr. I.D. Styliari, Dr. C. Conte, Dr. A. K. Pearce, Dr. A. Hüsler, Dr. R. J. Cavanagh, D. Gordhan, Dr. A. Nieto-Orellana, Dr. B. Couturaud, Prof. P. Williams, Dr. A. L. Hook, Prof. M. R. Alexander, Prof. M. C. Garnett, Prof. C. Alexander, Prof. J. C. Burley and Dr. V. Taresco
School of Pharmacy, University of Nottingham, University Park, Nottingham NG7 2RD, U.K.
E-mail: jonathan.burley@nottingham.ac.uk, cameron.alexander@nottingham.ac.uk
vincenzo.taresco@nottingham.ac.uk.

Dr. M. J. Limo

Interface and Surface Analysis Centre, University of Nottingham, School of Pharmacy, University Park, Nottingham, NG7 2RD, UK.

Prof. J. Suksiriworapong
Department of Pharmacy, Faculty of Pharmacy, Mahidol University, Ratchathewi, Bangkok 10400, Thailand

I.D.S. currently with School of Life and Medical Sciences, University of Hertfordshire, College Lane, Hatfield, AL10 9AB, UK

C.C. currently with Department of Pharmacy, University of Napoli Federico II, Napoli, 80131, Italy

B.C. currently with Department of Chemistry, University of Warwick, Gibbet Hill Road, CV4 7AL, UK.

Keywords: self-assembling; ink-jet printer; high throughput-miniaturized screening; nanoparticles

Abstract

The self-assembly of specific polymers into well-defined nanoparticles (NPs) is of great interest to the pharmaceutical industry as the resultant materials can act as drug delivery vehicles. In this work a high-throughput method to screen the ability of polymers to self-assemble into nanoparticles (NPs) using a picoliter ink-jet printer is presented. By dispensing polymer solutions in DMSO from the printer into the wells of a 96-well plate, containing water as an

antisolvent, we screened 50 suspensions for nanoparticle formation rapidly using only nanoliter to microliter. A variety of polymer classes were used, and in situ characterization of the sub-microliter nanosuspensions showed that the particle size distributions matched those of nanoparticles made from bulk suspensions. Dispensing organic polymer solutions into well-plates via the printer was thus shown to be a reproducible and fast method for screening nanoparticle formation which uses two to three orders of magnitude less material than conventional techniques.

Finally, a pilot study for a high-throughput pipeline of nanoparticle production, physical property characterization and cytocompatibility demonstrated the feasibility of the printing approach for screening of nano-drug delivery formulations. Nanoparticles were produced in the well plates, characterised for size and evaluated for effects on metabolic activity of lung cancer cells.

1. Introduction

Over the last few decades, the application of nanotechnologies to the biomedical and pharmaceutical field has significantly enhanced global health, improving diagnosis and treatment of several diseases.^{[1],[2]} A plethora of different materials has been used to produce nanosized carriers, from biodegradable polymers and lipids up to inorganic materials, and to date 51 nanoparticle (NP) formulations have been approved by the FDA for clinical applications (e.g. *Neulasta*, *Copaxone*^[3]). However, NP formulations can be challenging as there is a constant need to establish both functional and novel chemical and technological approaches in order to i) optimize the self-assembly behaviour of the base materials into NPs; ii) control and establish the reproducibility of the size, shape and colloidal behaviour of the NPs in accordance to the needs of the biomedical application; iii) modulate the encapsulation and the release rate of well-defined drugs and iv) minimise the use of surfactants and organic solvents in the preparation process. To address some of these needs, much interest has been focused on

amphiphilic block copolymers due to their versatility, their tunable properties and their ability to self-assemble into various types of NPs (micelles, nanospheres, nanocapsules and polymersomes).^{[4],[5],[6]} A range of different preparation techniques can be used, with typical polymeric NP preparation techniques involving in situ precipitation and solvent displacement, where the polymeric NPs self-assemble in the presence of a solvent (usually water), which is unfavourable for one block of the amphiphilic polymer. Such methods reduce the need of surfactants in the formulation process and utilise water-miscible solvents that can be easily removed if required.

Nevertheless, conventional methods need materials in the milligram scale, require days for the full removal of the solvent, face issues with scalability and batch-to-batch variability and frequently result in NPs with wide size distributions. Employing more sophisticated technologies to test new materials in an easy, fast and automated way that will enable the modulation of the NPs properties is still an unresolved challenge in this field. In this context, there is a real need for high throughput technologies to screen rapidly a large number of materials and optimise their formulation conditions. For example, the use of inkjet technology to obtain polymeric microspheres with defined sizes,^[7] protein encapsulated polymeric microstructures^[8] and loaded drug-polymer micro-particles^[9] has been well established in the literature. On this basis, inkjet printing could potentially be a promising alternative to the conventional methods used for the production of NPs. Inkjet printing is a versatile, scalable and relatively inexpensive method of depositing small volumes of solutions, even down to the picoliter range, with remarkable accuracy and reproducibility. As inkjet printers become more commercially available, their use in the field of drug delivery has increased.

Different materials have been printed by inkjet systems spanning from cells,^[10] to genes^{[11],[12]} or proteins^[13] to polymers^[14] to nanomaterials and some pharmaceutical formulations.^{[15],[16],[17]}

In a singular and pioneering work by Hauschild *et. al*,^[15] unilamellar nano-vesicles were printed from a conventional desktop inkjet printer, using ethanol solutions of both lipid-like and

amphiphilic copolymers, resulting in NPs with reproducible sizes ranging between 50 and 220 nm. In the same work, it was also shown that fluorescein loaded vesicles with narrow-size distributions could be directly produced via the printing method.^[15] However, in the literature, preparation of these NPs with the use of a conventional desk-top inkjet printer required solution volumes at the scale of 1 mL, similar to the ones needed for conventional individual batches prepared manually. While Hauschild *et.al* suggested that the inkjet NP-fabrication method would be relatively easy to integrate within a high-throughput platform, no reports to date exist in which ink-jet printing has been adopted to rapidly screen polymers able to self-assemble in water by using nano-to-micrograms of materials.

Therefore, in the present work we show a high-throughput, fast, reproducible and automated method to screen the self-assembling properties of different polymers into nanoparticles. The screening is accomplished via a 2-D picolitre-capable ink-jet printer dispensing polymer solutions into an anti-solvent (water) by using few microgram of final materials, contained in a 96-well plate system. We have employed a wide range of readily available commercial polymers, as well as some customised polymers from our own laboratories. Polymers with different architectures, linear block copolymers and grafted copolymers (polymer properties described in Table 1), were screened by using only micro-amounts/volumes (for a final NP concentration of 500 $\mu\text{g}/\text{mL}$ only 100 μg of polymer was required in 10 μL of DMSO dispensed in around 10 s in 200 μL of water) to evaluate their ability to self-assemble and to measure their size in different concentrations. All the concentrations were chosen based on previously published methods shown to allow polymer chains to self-assemble in water, and the data for these polymers were compared against appropriate control materials.^{[18],[19]}

The versatility of the ink-jet printing technology presented here as a miniaturized screening method may have implications for multiple pharmaceuticals platforms.

In this regards, Giardiello *et al.*^[20] developed an accelerated nanomedicine platform to generate a potential aqueous paediatric HIV nanotherapy, targeting oral dose, with clinical translation

and regulatory approval for human evaluation. Giardiello's small-scale screening used 1 mg of drug compound, generating large libraries of solid drug nanoparticles (160 individual components), and iterative pharmacological and chemical evaluation established potential candidates for progression through to clinical manufacture. The inkjet NP-fabrication method of the present work might be employed as a miniaturized pre-formulation screening step to be integrated within the work of Giardiello reported above or within general accelerated nanomedicine platform approaches where nanodispersions are screened as a valuable alternative to molecular solutions.^[21]

Finally, as a case study for a high throughput pipeline for nanoparticle production, characterization and effects on cell metabolic activity, a small experiment with selected polymers was performed. This proof-of-concept 'on-line assay' demonstrated the feasibility of the printing approach to screen formulations, from nano-particle preparation to preliminary cytotoxicity assays in a high-throughput fashion.

2. Results and Discussion

2.1 Validation of the use of ink-jet printing as a miniaturized methodology to screen polymers self-assembling in water by means of traditional analysis.

2.1.1 Known block-copolymer structures (*mPEG-b-PCL*, *mPEG-b-PLGA* and *mPEG-b-PεDL*)

Block co-polymers widely used in the drug delivery field such as *mPEG-b-PCL* and *mPEG-b-PLGA*,^{[22],[23],[24]} well-known to self-assemble in water into NPs, were first used to test the usefulness of the ink-jet printer as a NP formation screening technique. *mPEG-b-PCL* and *mPEG-b-PLGA* (50/50) were initially analysed at one single concentration (**Figure 1a**). Subsequently, to evaluate the reproducibility of the printer, replicates of *mPEG-b-PLGA* (50/50) were dispensed at different concentrations (**Figure 1-c** and SI). Moreover, a third block copolymer, *mPEG-b-PεDL*, with the hydrophobic part derived from renewable sources,^[25,26] thus, a convenient “green” replacement for PCL, was dispensed at two different concentrations in duplicate during the first set of experiments. Consistent reproducibility of *mPEG-b-PLGA* samples in terms of size distribution was observed and a similar trend with the common individual manual NP sample preparation method was also observed (SI, **Tables 1** and **2** for the reproducibility experiments).

Contrary to some typical nanoparticle preparation protocols, where the nanoparticle suspension is filtered for the removal of any aggregates, we did not filter the solutions containing the fabricated nanoparticles prior to the analysis, due to the small amount of suspension produced in the 96-well plate system. Thus, at the stage of the light scattering measurements, formation of precipitates during the measurements were noted (see correlograms and intensity distributions in SI, SI-Figure 3 and SI-Figure 4). Further manual/conventional experiments were performed, neglecting the filtration step, in order to investigate the ability of our method to mimic any events occurring at the larger mg scale. Consistently, aggregates were observed also in this latter conventional way to produce NPs (**Figure 1d**). In order to probe better these

common outcomes, a comparison with literature of similar polymeric structures in terms of chemistry and NP formation technique was established. In previously published work,^{[19], [27]} the ability of mPEG-*b*-PCL and PEG-*b*-PεDL to self-assemble and produce micelles was tested by dissolving the copolymers in acetone and adding the organic solutions at a fixed rate into HPLC grade water by using a pump system (each set of experiments involved 50 mg of polymer). Once the acetone was removed by slow evaporation under constant stirring, the micellar nano-suspensions were subsequently filtered through a membrane syringe filter (pore size: 220 nm) (Millex-LG, Millipore Co., USA) in order to remove aggregates and impurities formed during the self-assembling mechanism.^{[19], [28], [29]} We found possible formation of aggregates of similar materials by the printed method as well, where just a few μg were used instead of the 50 mg used in the existing literature.

2.1.2 PGA and its derivatives tested and compared to manual experiments

Further investigations were performed using Poly(glycerol-adipate) (PGA)^{[30], [31]} and some of its modifications (**Figure 2a**) as a polymeric platform. PGA is an amphiphilic polymer, which can be enzymatically synthesised from divinyl adipate and glycerol, with a tunable amount of branches along the main backbone.^[30] Due to its intrinsically non-toxic amphiphilic nature, this kind of polyester has been further functionalized to engineer new polymeric platforms for nanotechnology in the healthcare field. In particular, it has been further modified with biological molecules such as fatty acids and amino acids in order to enhance drug protein or nucleic acids interactions or encapsulation, or simply to tailor its hydrophobic-hydrophilic balance.^{[30], [31], [32]} PGA derivatives, including the bare polymer, showed molecular weights in the order of 20000 Da and all the materials were found to present an amorphous behaviour with T_g transitions ranging from -33 to 49 °C (see also Table 1).^[18] Full characterisation of these

polymers has been published in the past^[18] and for this reason is not included in this present work.

Unmodified and amino-acid modified (N-acylated Phenylalanine and N-acylated Tryptophan) PGAs, dispensed in various concentrations, formed well defined nanoparticles with hydrodynamic diameters in the range of 50 nm to 150 nm (**Figure 2b**). The diameter of the particles fabricated by the printer showed a similar trend to those prepared by the traditional manual method (Table 2) although some variance in final size values can be appreciated. These alterations may be attributed to several variables such as the lack of stirring in the printing step, the different rate of addition of the polymeric solution in water and the relative kinetics of solvent mixing. All the modified PGA adopted in the present work had 50% mol/mol average ratio of functionalisation.

PGA-Phe and PGA-Trp were also re-printed thrice to estimate the reproducibility of the methodology with these grafted polymers. As can be seen from **Figure 3** and Table 2 both sizes and PDIs were consistent by the DLS measurements.

In the attempt to assess the shape of some printed NPs in the dry state, we used TEM imaging. DLS allows the evaluation of the solvated NPs' size, where the values reported correspond to the NPs hydrodynamic diameter and as such are affected by solvent molecules associated to the nanomaterials, while TEM facilitates measurement of the dry and thus more compacted state of the nanoparticles.

PGA Trp (54 ± 11 nm, SI-Figure 16a) and PGA Phe NPs (77 ± 18 nm, SI-Figure 16b) showed a distribution of circular shaped NPs by TEM. As expected the dry diameter sizes are different from the ones recorded by DLS (PGA Trp 64 ± 1 nm and PGA Phe 133 ± 1 nm). It can also be seen that some of the particles do not show a well-defined spherical shape. We speculate that this effect is due to the partial evaporation of DMSO from the TEM specimen due to lack of further treatment, such as dialysis, as in common NPs formulation approaches. Nevertheless, TEM pictures showed a similar trend of DLS in final particles sizes behaviour, where PGA Trp

NPs were smaller than PGA Phe NPs and provided a promising first insight into the adoption of the printing methodology as a screening technique for pre-formulation steps. These size differences between these two techniques are large but consistent and it is a phenomenon that is well established and reported.^[33]

2.1.3 Large scale batch experiments

To further validate the printing screening approach, a larger scale batch experiment was performed. PGA was employed as a model system in the fabrication of 60 samples at two different concentrations (50 and 100 $\mu\text{g/mL}$) in one single printing event that required less than 20 minutes to be completed. All the samples were contained in a single well-plate and sizes were measured directly in a DLS plate-reader. It can be observed from **SI-Figure 17** that the printing batch-screening showed a good reproducibility in terms of sizes and particle distributions at the two explored concentrations. Interestingly, despite the similarity in concentration values, it is possible to evaluate differences in sizes with a marginal deviation between the two values, 71 ± 4 nm for the 100 $\mu\text{g/mL}$ and 65 ± 2 for the 50 $\mu\text{g/mL}$. This additional experiment may confirm the use of a printer to direct the self-assembling of amphiphilic materials in a large scale, such as for industrial batch-screening.

2.1.4 Negative printing controls and validation of method

Negative “printing” controls were also performed using polymers that were not expected to self-assemble once dispensed in water without the use of a second surfactant,^{[34],[35]} PVP and PVPVA demonstrated very poor correlation on the DLS (**Figure 4**). These latter sets of

observations highlight the possibility to distinguish between materials able to self-assemble in water and those which do not self-assemble, thus avoiding any “false-positive” results.

2.2 Case study scenario: NPs production, self-assembling screening and biological response of selected polymeric materials in high-throughput fashion.

A pilot study investigating a high throughput pipeline of printed nanoparticle production, characterization and cell-based screening was performed. The above experiments were repeated on a small scale in an entirely high-throughput fashion, with the intention that this process may be translated as an example to validate the use of polymers as a carrier for drug delivery formulations. Five samples were chosen for the study: three PGA variants (namely PGA, PGA Phe and PGA Trp) as well as two negative control polymers (PVP and PVPVA) that previously were found not to self-assemble. All the materials were printed in a well-plate containing water at two different concentrations (50 and 250 $\mu\text{g}/\text{mL}$) and were directly analysed for their self-assembling ability by a high throughput DLS plate reader (HT-DLS). To corroborate the concept of pipeline screening a high throughput cell cytotoxicity assay (MTS) was carried out directly on the printed samples without any further or intermediate purifications.

The HT-DLS data of the printed versus the samples prepared in bulk revealed a similarity in the sizes obtained for all the PGA variant polymers was noticed (**Figure 5** see also **SI-Figure 18**). Two trends were observed for both the NP preparation techniques adopted. Both PGA-Phe and PGA-Trp at the two explored concentrations showed sizes bigger than pure PGA NPs. At the same time, a clear enlargement of NPs sizes for all the explored materials was observed on increasing the concentration from 50 $\mu\text{g}/\text{mL}$ to 250 $\mu\text{g}/\text{mL}$.

Cytotoxicity is of critical importance for the clinical translation of any kind of nanosized carrier. The formulation strategies employed for NPs production, including the presence of surfactants and of course of solvent traces, significantly affect cell metabolism. In our formulations, the

concentration of DMSO in the final nanosuspensions was determined to be non-cytotoxic (**Figure 6**), in agreement with previous evidence.^[36] In fact, as evident in **Figure 6**, the different NP formulations obtained by printing, did not show any negative effects on the metabolic activity of H1299 lung cancer cells after 24h of treatment, in line with the data reported for NPs made by similar polymers but through different formulation processes.^[36] Therefore, the high throughput method of directly transferring the formulations in the well plates to any cell-based assays required, including cytotoxicity assays, has been validated. It should be noted that previous literature has shown that PGA and its derivatives are not toxic (although different cell lines have been used in previous works).^{[18],[31],[37]}

Taking this into consideration, the successful *in vitro* application of different polymers reported throughout the present manuscript was validated. The polymers selected had different structures, molecular weight distributions and amphiphilic properties. Both size measurement distributions and repeat sequences of negative controls showed an excellent match with manually-prepared nanosuspensions. At the same time, the precision of the system allowed the fast and accurate calculation of the number of droplets needed to achieve the final polymer concentrations. The suitability and versatility of the technology presented here as a miniaturized screening method may have implications for multiple pharma and medical platforms.

3. Conclusions

The results presented support the adoption of inkjet printing as a high throughput NP formulation investigation method, with the key strengths of the method lying in the automation, low amounts used, and reproducibility. To probe the self-assembling behaviour of any of the materials tested in the present work at the final concentration of 1 mg/mL (in triplicate), a total

of 600 μg of polymer was required. This could be dispensed in a few minutes without any human intervention (see Calculation sheet). The rapid addition of small amounts of polymer-DMSO solution allowed the quick diffusion of the DMSO without the need for mechanical stirring and thus the controlled formation of the NPs.

Known block copolymers such as mPEG-*b*-PCL and mPEG-*b*-PLGA were initially used, as models, to explore the ability of an ink-jet printer to produce NPs inside a well-plate. The printed NPs showed good reproducibility throughout the sample polymer set and a close match with the particles prepared manually. Interestingly, although a limited amount of material was used, it was possible to link aggregate formation with the mg scale samples formed by the conventional method, which is consistent with evidence of aggregation previously reported in literature. By adopting the same nozzle/instrument conformation it is also possible to use solvents such as water, DMF, DMSO and mixtures with low boiling point solvents. However, for the scope of screening the self-assembling of materials mimicking a nanoprecipitation process, there are two key advantages in the selection of DMSO as solvent. DMSO is water miscible, allowing the nanoparticle formation via solvent displacement to take place, and DMSO has a high boiling point to avoid nozzle clogging. DMSO is also the most common solvent used in the drug discovery field to dissolve, screen and store the thousands of compounds synthesized and designed by combinatorial chemistry.^[38] Additionally, the adoption of the ink-jet printer to probe the ability of polymer chains to self-assemble in NPs showed remarkable advantages, including the use of limited amounts of materials, full automation, low amount of waste, reduction of toxic solvents, fast screening and miniaturized storage. In fact, taking into account this latter variable, all the printed samples explored in the present work (over 100, considering all the replicates) were stored in a couple of 96 well-plates while the same samples prepared manually needed to be stored in as many vials as number of wells to match the full comparison. Not only, the reduction of storage space renders this technique extremely appealing in terms of easy allocation and sample/data retrieval. Even on

the repeat printing sequences of the negative controls (PVP and PVPVA) the results were completely reproducible.

Finally, a pilot study of high throughput pipeline of nanoparticle production, characterization and cell assay demonstrated the feasibility of the printing approach for screening of nanodrug delivery formulations. We believe the high throughput self-assembly characterisation via 2D inkjet printing has the potential to become a standard method for particle engineering and rapid formulation development.

4. Experimental Section

4.1 Printing set-up and work flow conditions

Prior to dispensing the DMSO polymer solution into a 96-well plate filled with antisolvent (water, 200 μ L per well), the target had to be programmatically defined. Firstly, the outer dimensions of the plate were added to the software sciFLEXARRAYER (Scienion AG, version 2.09.002) followed by defining the number of wells, well distance, well depth and the spot area (area within the target designated for spotting). Within the spot area, a field pattern was defined as a 9x9 spot matrix. After setting up the field pattern, the field setup was used to address the wells from the probe substrate to the spots. The probe substrate consists of the well plate containing the polymer solution with a starting concentration of 10 mg/mL (Scheme 1(A)). DMSO polymer solutions were dispensed via a piezo electric inkjet printer (Sciflexarray S5, Scienion) using a 90 μ m orifice nozzle. The nozzle was programmed to dispense the DMSO polymer solutions into the well from a vertical distance of *circa* 10-20 mm from the well-plate, without touching the water surface. In all experiments, 25 spots in the defined field (Scheme 1 B, highlighted in light green) were selected as the “print pattern”. The droplet size was controlled by the values of the voltage and electrical pulse. The voltage and electrical pulse were also tuned to prevent the occurrence of satellite droplets (see Support Info, SI-Figure 1, SI-Figure 2). Images of the drop formation and droplet size were obtained using the printer

software. The final spots were imaged using the Leica MZ16 stereomicroscope. Depending on the concentration to be reached, the number of drops per spot was adjusted accordingly; for example, 1000 drops (each drop shows a volume in between 360 and 400 pL dispensed every 30 μ s) per spot for 2.0 mg/mL and 3 drops per spot for 0.001 mg/mL. The number of drops per spot were selected in such a way that the volume aspired by the nozzle (max 10 μ L) in the beginning of a run was sufficient to dispense the whole targeted final concentration of nanoparticles in the water volume in the well. Therefore, a multitude of runs were printed into the same well in order to achieve the desired polymer concentration. The amount of polymeric material used in the experiments is one of the strongest points of the method. In a routine experiment DMSO solution (10 mg/mL) droplets with nominal volumes ranging from 360 pL to 400 pL were dispensed into the targeted well filled with water, at a 300 Hz jetting frequency by adjusting the voltage and pulse between 98 V to 109 V and 53 μ s to 65 μ s, respectively (see Support Info). The nozzle was washed with DMF, in between each printing cycle, as part of the automated printing/washing loop. Once DMSO solutions were printed, the fast diffusion of the organic solvent into water drove the self-assembling of the polymers. DMSO was chosen both due to its high evaporation point that avoids clogging of the printer nozzle^[39], because it is water miscible and also because it acts as a common solvent for many drugs and polymers^{[40],[38]}. For the investigation of the NP formation at the highest polymer concentration of 2 mg/mL, the amount of polymer needed for the printing was 400 μ g, while in a conventional nanoprecipitation this is typically up to 10 mg or more.

4.2 Traditional methodology: manual preparation

A subset of nanoparticle suspensions were prepared following a protocol previously established^[33] (final NPs concentration equal to 2 mg/mL): 2 mL of a stock solution of polymer in organic solvent (DMSO, with the exception of mPEG-*b*-PCL where a mixture of DMSO:Acetone in 50:50 % vol/vol was adopted) were added dropwise to 5 mL of filtered water

(HPLC-grade). The solution was left overnight under constant gentle stirring for the evaporation of the organic solvent, when the final nanosuspension was collected for size analysis via DLS. This procedure required approximately 10 mg of polymer for each final suspension, 2 mL of DMSO, 5 mL of water and lasted approximately 24 hours. Every single NPs suspension needed to be stored in a vial. In comparison, the same experiment performed by ink-jet printing required 0.4 mg of polymer, 40 μ L of DMSO and 200 μ L of water. This latter sample was confined to one single well of a 96-well plate.

4.3 Nanoparticle Size Analysis

Dynamic Light Scattering (DLS) measurements were conducted in triplicate on the final unfiltered nanosuspensions, produced both manually and printed, using a Malvern Zetasizer Nano ZS at 25°C (scattering angle 173°, laser of 633 nm). TEM samples were prepared as follows; the sample in aqueous suspension (13 μ L) was added to a copper grid (Formvar/Carbon film 200 mesh Copper (100)). The sample was left on the grid for 10 minutes and then the excess was removed using filter paper. Then, freshly prepared uranyl acetate (2%, 13 μ L) was added on the grid and was left for 5 minutes before the removal of the excess with filter paper. The grid was allowed to dry under a fume hood for a minimum of 30 minutes prior to use. TEM images were captured using the FEI Biotwin-12 TEM equipped with a digital camera at the Nanoscale and Microscale Research Centre (NMRC) of the University of Nottingham. TEM image analysis for the size distribution of the NPs was performed via ImageJ (version 1.51j8).^[41]

4.3.1 Particle Size Characterization using High Throughput Dynamic Light Scattering (HT-DLS)

Particle size analysis of the final unfiltered nanosuspensions, produced both manually and printed was performed using a Wyatt DynaPro Plate Reader II DLS instrument which has a

laser wavelength of 817.28 nm and a scattering angle of 158°. Experimental temperature was set to 25 °C and auto attenuation was enabled to determine the optimal laser power and attenuation. For a measurement in each well containing 100 µL of sample, 10 acquisitions were carried out, each for 10 seconds. DYNAMICS software implementing the Dynals algorithm was used for the data analysis.

4.4 Metabolic activity

H1299 lung cancer cells were obtained from the American Type Culture Collection, cultured at 37°C in a humidified atmosphere containing 5% CO₂ and grown routinely in RPMI supplemented with 10% FBS, 100 unit/mL penicillin and 100 µg/mL streptomycin. H1299 cells were seeded at a density of 2×10^4 cells/well in 96 well plates and cultured in 100 µl RPMI medium containing 10% FBS for 24h prior to NP treatment. NP suspensions were applied in culture medium at a final concentration of 125 µg/ml for 24h.

Additionally, to study the cytocompatibility of the DMSO concentration present in the final NP dispersions, medium containing 0.75% (v/v) DMSO was applied to cells. Cells were also treated with 0.1% (v/v) Triton-X 100 and culture medium alone for 24h for use as positive and negative controls, respectively. Following treatment, cells were washed with PBS and incubated with 20 µl MTS solution (CellTiter 96® Aqueous One Solution Cell Proliferation Assay, Promega) diluted with 100 µl medium per well for 3h. Absorbance was then read at 490 nm in a microplate reader (Tecan Spark 10M, UK). Relative metabolic activity was calculated with the absorbance at 490 nm for the negative control set as 100%, and the positive control as 0%.

Acknowledgements

We thank Engineering and Physical Sciences Research Council (EPSRC; Grants EP/N03371X/1, EP/H005625/1, EP/N006615/1 and EP/L013835/1) and the Royal Society

(Wolfson Research Merit Award WM150086) for funding this work. Ioanna Danai Styliari acknowledges EP/I01375X/1. Claudia Conte was supported by a fellowship by Associazione Italiana per la Ricerca sul Cancro (AIRC) co-funded by the European Union (iCARE/Marie Curie 2014). Andrew Hook and Morgan Alexander acknowledge the Wellcome Trust (Senior Investigator Award ref: 103882). The authors acknowledge the Nanoscale and Microscale Research Centre (NMRC) of the University of Nottingham for access to TEM imaging. We thank the Interface and Surface Analysis Centre (ISAC) for carrying out the high throughput particle size analysis.

Data access statement

All raw data created during this research are openly available from the corresponding author (vincenzo.taresco@nottingham.ac.uk) and at the University of Nottingham Research Data Management Repository (<https://rdmc.nottingham.ac.uk/>) and all analyzed data supporting this study are provided as supplementary information accompanying this paper.

References

- [1] V. Wagner, A. Dullaart, A.-K. Bock, A. Zweck, *Nat. Biotechnol.* **2006**, *24*, 1211.
- [2] P. Couvreur, C. Vauthier, *Pharm. Res.* **2006**, *23*, 1417.
- [3] D. Bobo, K. J. Robinson, J. Islam, K. J. Thurecht, S. R. Corrie, *Pharm. Res.* **2016**, *33*, 2373.
- [4] K. Letchford, *Eur. J. Pharm. Biopharm.* **2007**, *65*, 259.
- [5] A. Rösler, G. W. . Vandermeulen, H.-A. Klok, *Adv. Drug Deliv. Rev.* **2001**, *53*, 95.
- [6] C. Vauthier, K. Bouchemal, *Pharm. Res.* **2009**, *26*, 1025.
- [7] T. Ehtezazi, N. M. Dempster, G. D. Martin, S. D. Hoath, I. M. Hutchings, *J. Pharm. Sci.* **2014**, *103*, 3733.
- [8] J. Xie, W. J. Ng, L. Y. Lee, C.-H. Wang, *J. Colloid Interface Sci.* **2008**, *317*, 469.
- [9] Y. Yeo, O. A. Basaran, K. Park, *J. Control. Release* **2003**, *93*, 161.
- [10] S. Umezu, T. Kitajima, H. Ohmori, Y. Ito, *Sensors Actuators A Phys.* **2011**, *166*, 251.
- [11] M. J. Heller, *Annu. Rev. Biomed. Eng.* **2002**, *4*, 129.
- [12] S. Venkatasubbarao, *Trends Biotechnol.* **2004**, *22*, 630.
- [13] B. H. Lee, T. Nagamune, *Biotechnol. Bioprocess Eng.* **2004**, *9*, 69.
- [14] A. Mant, G. Tourniaire, J. J. Diaz-Mochon, T. J. Elliott, A. P. Williams, M. Bradley, *Biomaterials* **2006**, *27*, 5299.
- [15] S. Hauschild, U. Lipprandt, A. Rumpelcker, U. Borchert, A. Rank, R. Schubert, S. Förster, *Small* **2005**, *1*, 1177.
- [16] W. S. Cheow, T. Y. Kiew, K. Hadinoto, *Eur. J. Pharm. Biopharm.* **2015**, *96*, 314.
- [17] H.-Y. Hsu, S. Toth, G. J. Simpson, M. T. Harris, *AIChE J.* **2015**, *61*, 4502.
- [18] V. Taresco, J. Suksiriworapong, I. D. Styliari, R. H. Argent, S. M. E. Swainson, J. Booth, E. Turpin, C. A. Laughton, J. C. Burley, C. Alexander, M. C. Garnett, *RSC Adv.* **2016**, *6*, 109401.
- [19] D. Kakde, V. Taresco, K. K. Bansal, E. P. Magennis, S. M. Howdle, G. Mantovani, D. J. Irvine, C. Alexander, *J. Mater. Chem. B* **2016**, *4*, 7119.
- [20] M. Giardiello, N. J. Liptrott, T. O. McDonald, D. Moss, M. Siccardi, P. Martin, D. Smith, R. Gurjar, S. P. Rannard, A. Owen, *Nat. Commun.* **2016**, *7*, 13184.
- [21] H. Zhang, D. Wang, R. Butler, N. L. Campbell, J. Long, B. Tan, D. J. Duncalf, A. J. Foster, A. Hopkinson, D. Taylor, D. Angus, A. I. Cooper, S. P. Rannard, *Nat. Nanotechnol.* **2008**, *3*, 506.
- [22] Z.-Y. He, K. Shi, Y.-Q. Wei, Z.-Y. Qian, *Curr. Drug Metab.* **2016**, *17*, 168.
- [23] A. Rosler, G. W. M. Vandermeulen, H. A. Klok, *Adv. Drug Deliv. Rev.* **2001**, *53*, 95.
- [24] N. Kumar, M. N. V. Ravikumar, A. J. Domb, *Adv. Drug Deliv. Rev.* **2001**, *53*, 23.
- [25] A. Endrizzi, Y. Pagot, A. Le Clainche, J. M. Nicaud, J. M. Belin, *Crit. Rev. Biotechnol.* **1996**, *16*, 301.
- [26] C. Romero-Guido, I. Belo, T. M. N. Ta, L. Cao-Hoang, M. Alchihab, N. Gomes, P. Thonart, J. A. Teixeira, J. Destain, Y. Waché, *Appl. Microbiol. Biotechnol.* **2011**, *89*, 535.
- [27] K. K. Bansal, D. Kakde, L. Purdie, D. J. Irvine, S. M. Howdle, G. Mantovani, C. Alexander, *Polym. Chem.* **2015**, *6*, 7196.
- [28] M. Gou, K. Men, H. Shi, M. Xiang, J. Zhang, J. Song, J. Long, Y. Wan, F. Luo, X. Zhao, Z. Qian, *Nanoscale* **2011**, *3*, 1558.
- [29] S. Galindo-Rodriguez, E. Allemann, H. Fessi, E. Doelker, *Pharm. Res.* **2004**, *21*, 1428.
- [30] V. Taresco, R. G. Creasey, J. Kennon, G. Mantovani, C. Alexander, J. C. Burley, M. C. Garnett, *Polymer (Guildf)*. **2016**, *89*, 41.
- [31] P. Kallinteri, S. Higgins, G. a. Hutcheon, C. B. St. Pourain, M. C. Garnett, *Biomacromolecules* **2005**, *6*, 1885.
- [32] V. M. Weiss, T. Naolou, G. Hause, J. Kuntsche, J. Kressler, K. Mäder, *J. Control.*

- Release* **2012**, 158, 156.
- [33] R. F. Domingos, M. A. Baalousha, Y. Ju-Nam, M. M. Reid, N. Tufenkji, J. R. Lead, G. G. Leppard, K. J. Wilkinson, *Environ. Sci. Technol.* **2009**, 43, 7277.
- [34] K. J. Frank, U. Westedt, K. M. Rosenblatt, P. Hölig, J. Rosenberg, M. Mägerlein, G. Fricker, M. Brandl, *J. Pharm. Sci.* **2014**, 103, 1779.
- [35] A. Dan, I. Chakraborty, S. Ghosh, S. P. Moulik, *Langmuir* **2007**, 23, 7531.
- [36] G. Da Violante, N. Zerrouk, I. Richard, G. Provot, J. C. Chaumeil, P. Arnaud, *Biol. Pharm. Bull.* **2002**, 25, 1600.
- [37] V. M. Weiss, T. Naolou, T. Groth, J. Kressler, K. Mäder, *J. Appl. Biomater. Funct. Mater.* **2012**, 10, 163.
- [38] R. J. Bastin, M. J. Bowker, B. J. Slater, *Org. Process Res. Dev.* **2000**, 4, 427.
- [39] V. Taresco, I. Louzao, D. Scurr, J. Booth, K. Treacher, J. McCabe, E. Turpin, C. A. Laughton, C. Alexander, J. C. Burley, M. C. Garnett, *Mol. Pharm.* **2017**, 14, 2079.
- [40] S. Balbach, C. Korn, *Int. J. Pharm.* **2004**, 275, 1.
- [41] C. T. Rueden, J. Schindelin, M. C. Hiner, B. E. DeZonia, A. E. Walter, E. T. Arena, K. W. Eliceiri, *BMC Bioinformatics* **2017**, 18, 529.

Figure 1. Hydrodynamic diameter distributions and Polydispersity indexes (PDI) of NPs formed from block copolymers: (a) mPEG-*b*-PCL and mPEG-*b*-PLGA NPs, formed via the printing method, at a final 0.5 mg/mL polymer in water concentration, (b) Cumulative graph of the size results of all the block copolymers used in this work in final concentrations of 0.5 mg/mL and 1 mg/mL. With aggregation of mPEG-*b*-PCL at 0.5 mg/mL the 1 mg/mL concentration was not printed. In both (a) and (b) the error bars correspond to the standard deviation of the three DLS measurements. (c) Intensity based size distribution, as measured via DLS, for the mPEG-*b*-PLGA NPs, at three different final concentrations. (d) Comparison of the mPEG-*b*-PLGA NPs size distributions, as formed via the printed (straight line) and the traditional hand method (dotted line) at a 2 mg/mL final polymer concentration.

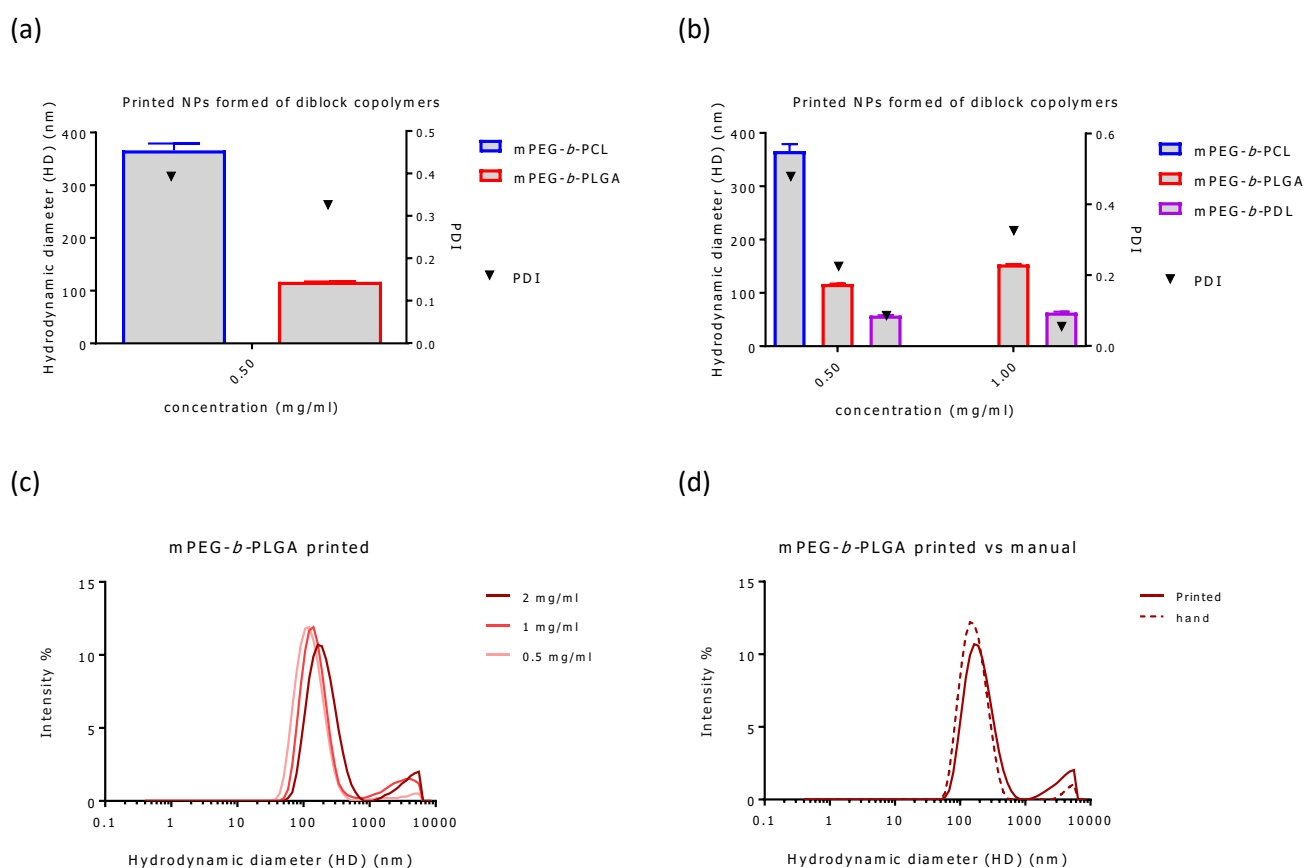
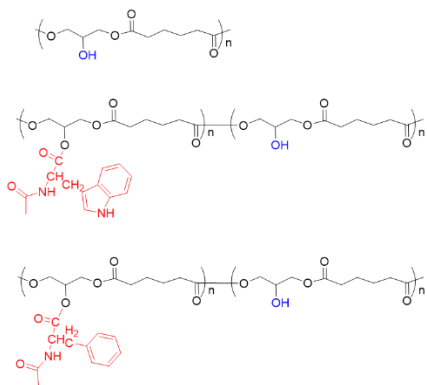


Figure 2. Investigation of forming NPs from PGA and PGA-modified polymers; (a) structures of the polymers, (b) comparison of sizes and PDIs between printed NPS and manually prepared by DLS. All the samples were prepared at 1 mg/mL as final suspension concentration in water.

(a)



(b)

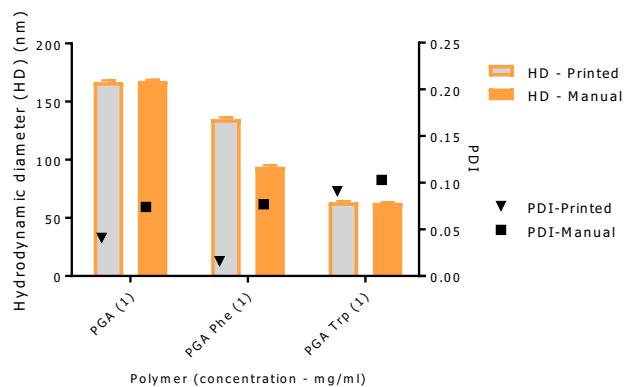


Figure 3. Batch reproducibility of nanoparticles formed by printing PGA-Trp and PGA-Phe polymers.

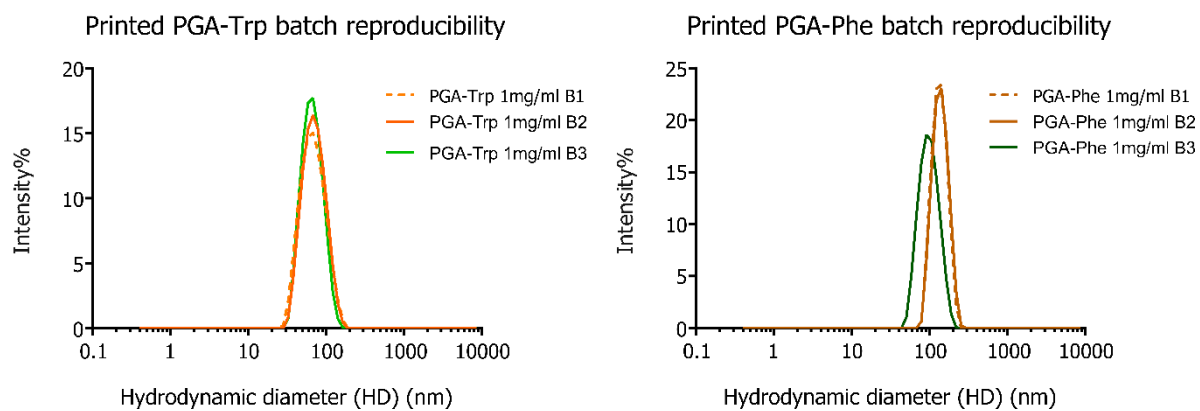


Figure 4. Raw intensity and correlation data for the printed PVP and PVPVA suspensions, used as a negative control in this work.

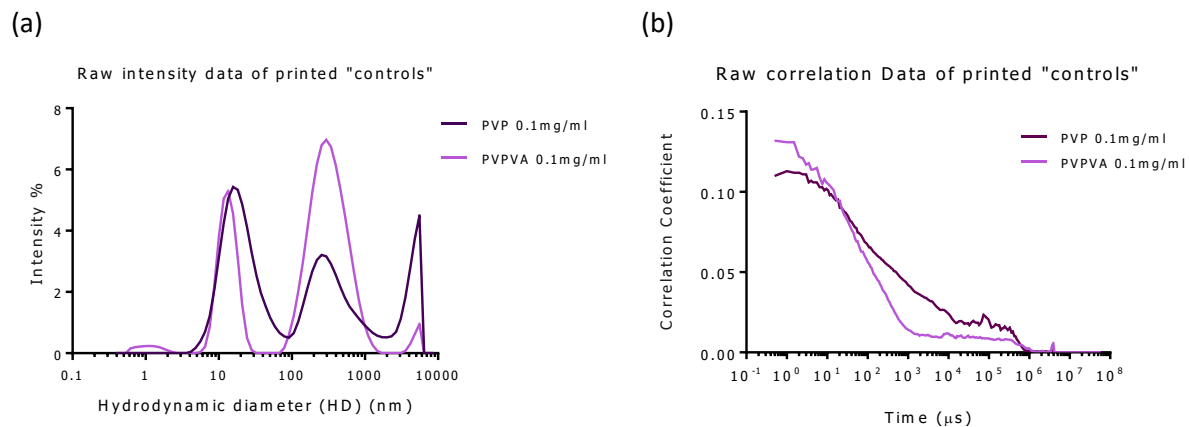


Figure 5. High throughput DLS particle size characterisation of the final unfiltered nanosuspensions of Poly(glycerol-adipate) (PGA), PGA-Phenylalanine (PGA-Phe) and PGA-tryptophan (PGA-Trp) synthesised by (A) printing and (B) manually by hand at 50 $\mu\text{g/mL}$ and 250 $\mu\text{g/mL}$ polymer concentration.

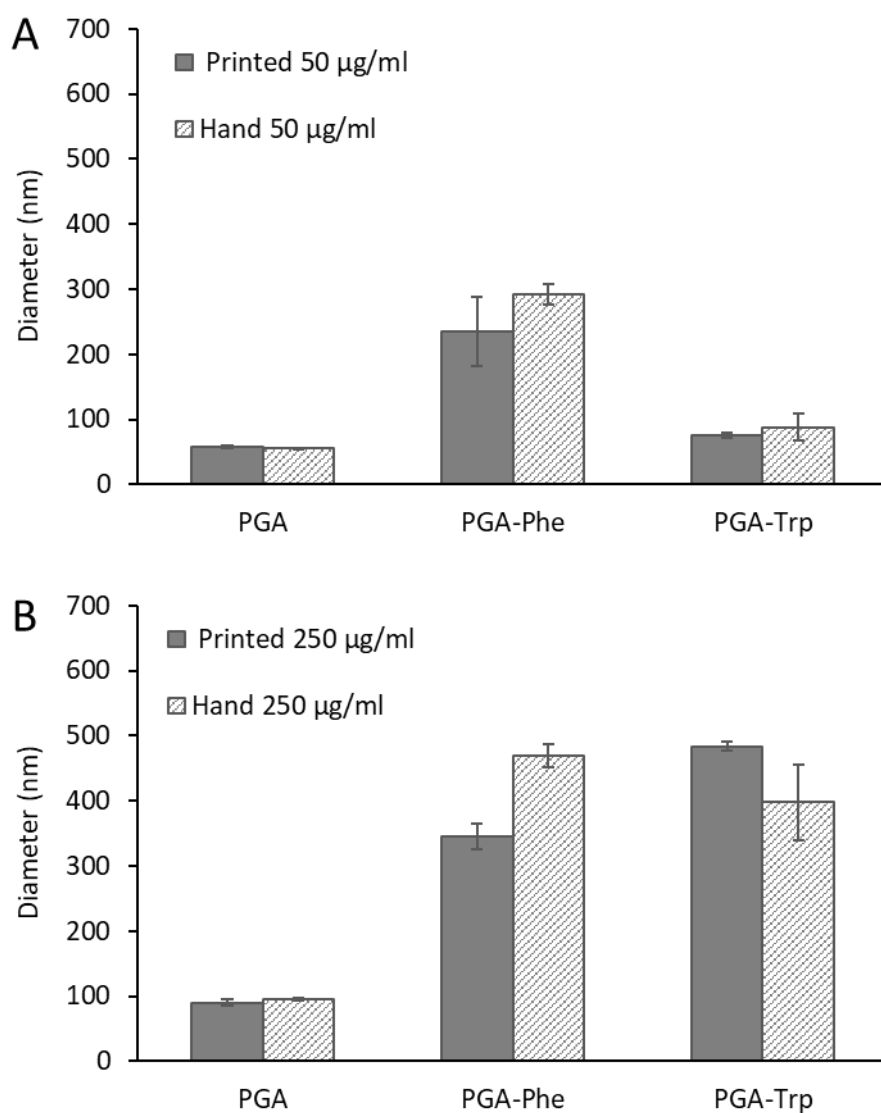
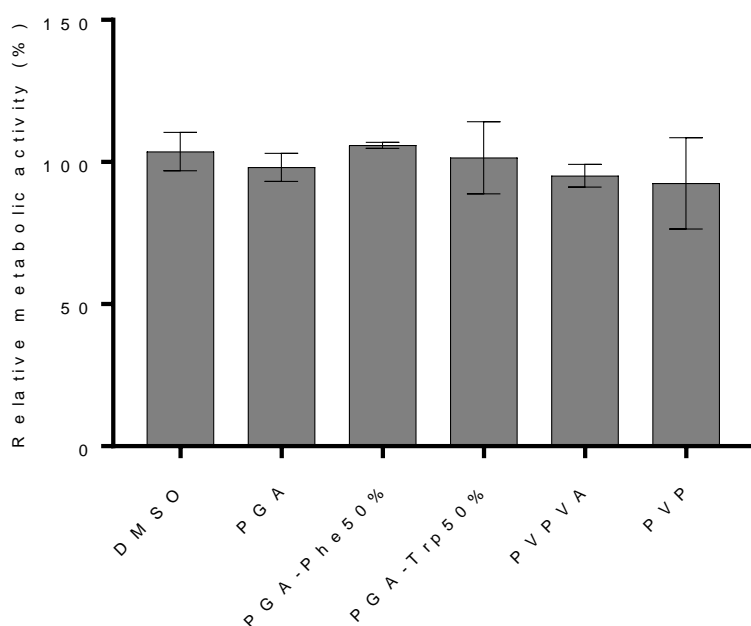


Figure 6. Cytotoxicity for selected polymers as determined by the MTS assay. H1299 cells were treated with polymers at a concentration of 125 $\mu\text{g/ml}$ or with 0.75% (v/v) DMSO for 24h. Data are presented as relative (%) values normalized to negative control (medium alone) and positive control (0.1% v/v Triton-X 100), set as 100% and 0%, respectively.



Scheme 1. (A) Printing process by focusing on the nozzle set-up. On the left-hand side, polymer solution aspiration. On the right-hand side printing/dispensing of the aspired polymer solution into wells filled with 200 μL of antisolvent (water). (B) 96-well plate as the target substrate,

detailed view of a well with designed spot area and field, selected print pattern with adjustable number of drops per spot in magnified view.

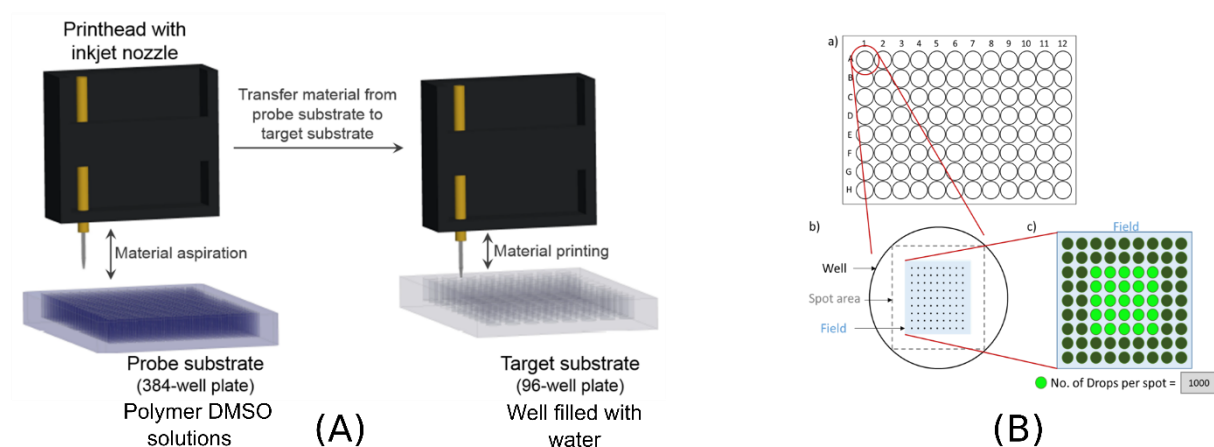


Table 1 – Table of the properties of polymers used. Molecular weight (M_n) and dispersity (\mathcal{D}) were calculated via GPC, while thermal properties (glass transition temperature, T_g and melting points T_m) were assessed using DSC.

Polymer	M_n (g mol ⁻¹)	\mathcal{D}	T_g	T_m
PGA ^[18]	19480	2.6	-33	-
PGA Trp ^[18]	25640	2.8	49	-
PGA Phe ^[18]	23980	2.2	12	-
mPEG- <i>b</i> -PeDL ^[19]	15000	1.1	-52	57
mPEG- <i>b</i> -PLGA	7900	1.3	-5	-
mPEG- <i>b</i> -PCL ^[19]	17000	1.5	-57	60

Table 2. Table of the Polyglycerol adipate polymers used, both in the printed and in the "traditional" manual nanoprecipitation method, and resulting NP sizes as measured by dynamic light scattering. Average size, polydispersity index and standard deviation values were calculated from 3 measurements.

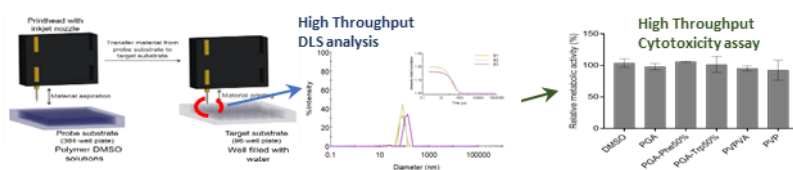
Polymer	Concentration (mg/ml)	Method	Hydrodynamic Diameter (nm) \pm SD	PDI \pm SD
PGA	1	Printed	167 \pm 1	0.041 \pm 0.022
		Manual	168 \pm 1	0.074 \pm 0.018
	0.5	Printed	94 \pm 1	0.046 \pm 0.003
		Manual	105 \pm 1	0.127 \pm 0.018
PGA-Trp	1	Printed	66 \pm 1	0.091 \pm 0.014
		Manual	63 \pm 1	0.092 \pm 0.016
	0.5	Printed	61 \pm 1	0.089 \pm 0.012
		Manual	57 \pm 1	0.036 \pm 0.006
PGA-Phe	1	Printed	132 \pm 2	0.016 \pm 0.006
		Manual	94 \pm 1	0.087 \pm 0.021
	0.5	Printed	123 \pm 2	0.018 \pm 0.007
		Manual	93 \pm 1	0.083 \pm 0.011

Ink-jet printing is employed as high throughput and miniaturized method to screen nanoparticles (NPs) formulations. Polymer solutions are swiftly dispensed into well-plates using two to three orders of magnitude less material than conventional state-of-the-art techniques. The formation of NPs, their sizes and their cytocompatibility are directly assessed in a single well-plate format, minimizing human-errors and batch variability, and providing pilot data to assist nanoparticle selection and manufacture.

Keyword: self-assembling, ink-jet printer, high throughput-miniaturized screening, Nanoparticles

Ioanna D. Styliari, Claudia Conte, Amanda K. Pearce, Amanda Hüsler, Robert J. Cavanagh, Marion J. Limo, Dipak Gordhan, Alejandro Nieto-Orellana, Jiraphong Suksiriworapong, Benoit Coutraud, Phil Williams, Andrew L. Hook, Morgan R. Alexander, Martin C. Garnett, Cameron Alexander*, Jonathan C. Burley* and Vincenzo Taresco*

High throughput miniaturized screening of nanoparticle formation via inkjet printing



Supporting Information

High throughput miniaturized screening of nanoparticle formation via inkjet printing

Ioanna D. Styliari, Claudia Conte, Amanda K. Pearce, Amanda Hüsler, Robert J. Cavanagh, Marion J. Limo, Dipak Gordhan, Alejandro Nieto-Orellana, Jiraphong Suksiriworapong, Benoit Couturaud, Phil Williams, Andrew L. Hook, Morgan R. Alexander, Martin C. Garnett, Cameron Alexander, Jonathan C. Burley* and Vincenzo Taresco**

Dr. I.D. Styliari, Dr. C. Conte, Dr. A. K. Pearce, Dr. A. Hüsler, Dr. R. J. Cavanagh, D. Gordon, Dr. A. Nieto-Orellana, Dr. B. Couturaud, Prof. P. Williams, Dr. A. L. Hook, Prof. M. R. Alexander, Prof. M. C. Garnett, Prof. C. Alexander, Prof. J. C. Burley and Dr. V. Taresco
School of Pharmacy, University of Nottingham, University Park, Nottingham NG7 2RD, U.K.
E-mail: jonathan.burley@nottingham.ac.uk, cameron.alexander@nottingham.ac.uk
vincenzo.taresco@nottingham.ac.uk.

Dr. M. J. Limo

Interface and Surface Analysis Centre, University of Nottingham, School of Pharmacy, University Park, Nottingham, NG7 2RD, UK.

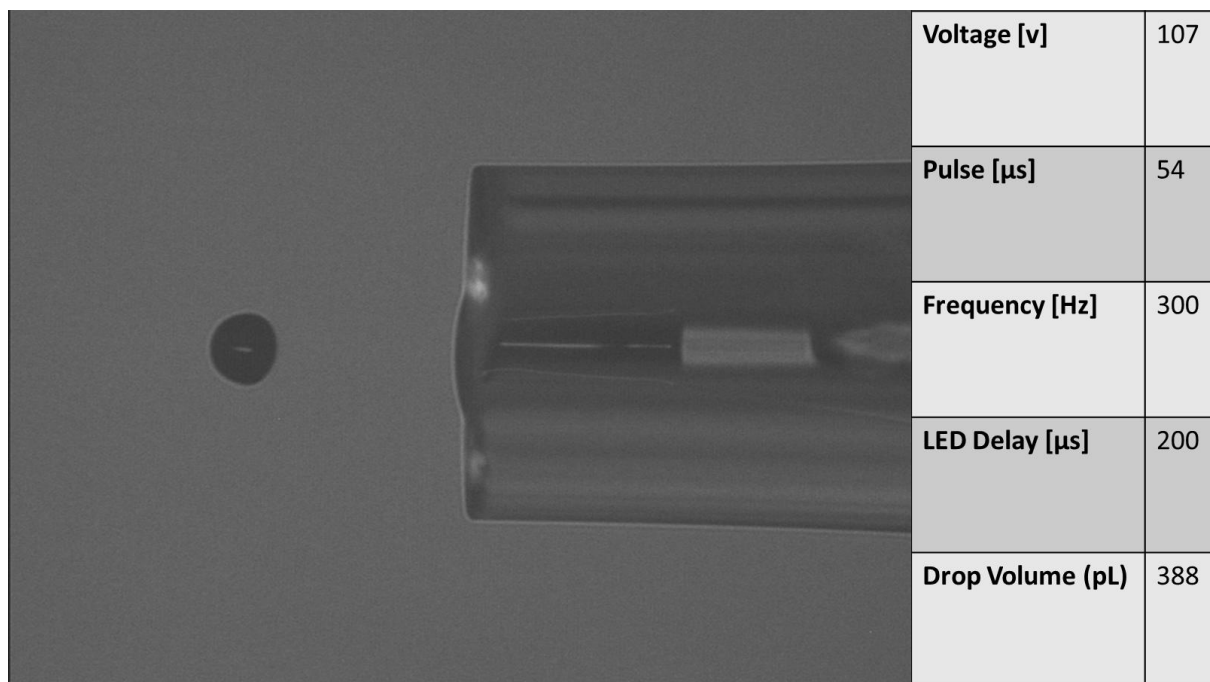
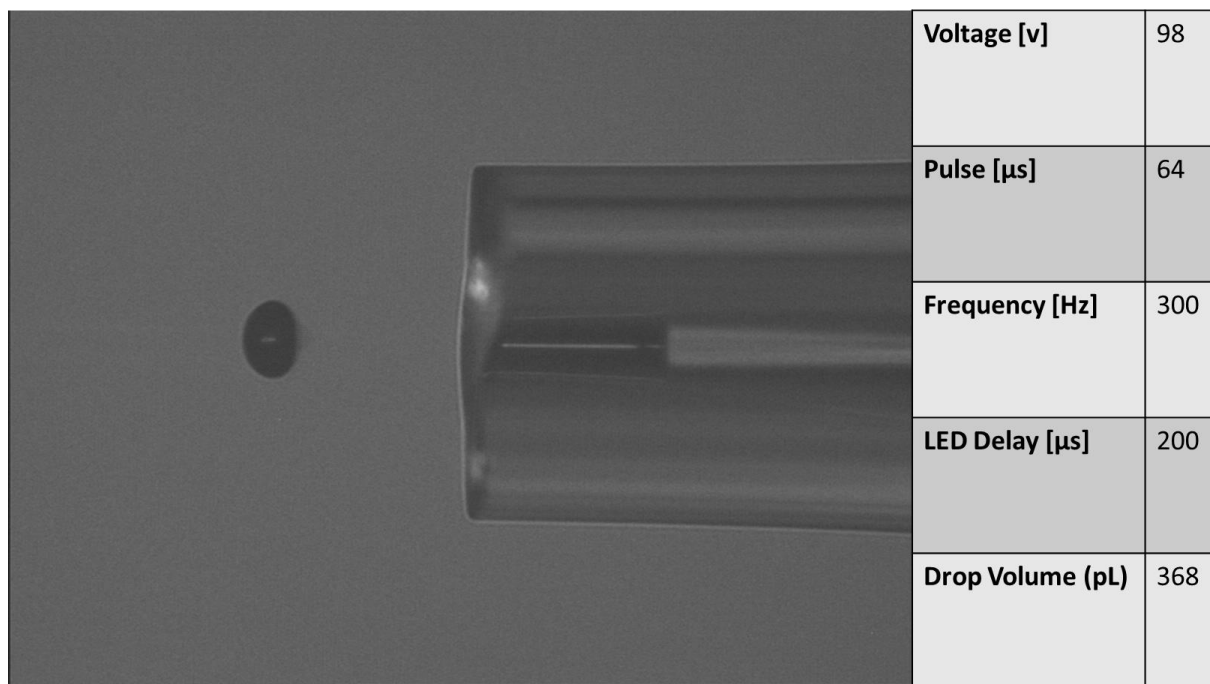
Prof. J. Suksiriworapong
Department of Pharmacy, Faculty of Pharmacy, Mahidol University, Ratchathewi, Bangkok 10400, Thailand

I.D.S. currently with School of Life and Medical Sciences, University of Hertfordshire, College Lane, Hatfield, AL10 9AB, U.K

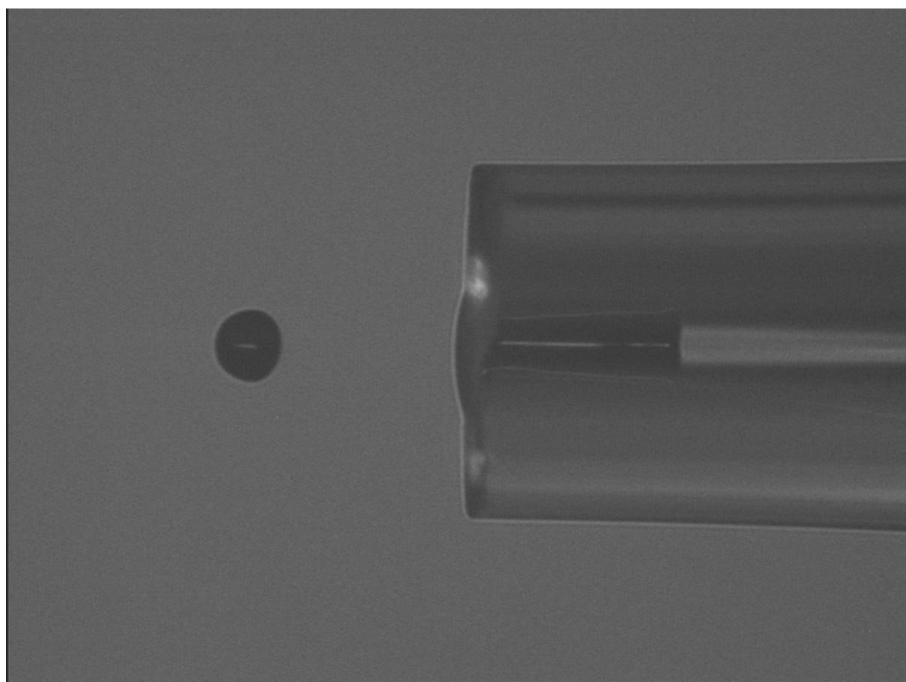
C.C. currently with Department of Pharmacy, University of Napoli Federico II, Napoli, 80131, Italy

B.C. currently with Department of Chemistry, University of Warwick, Gibbet Hill Road, CV4 7AL, UK.

SI-Figure 1. Droplet Size and Printing information for the PGA, PGA Trp and PGA Phe printed NPs.

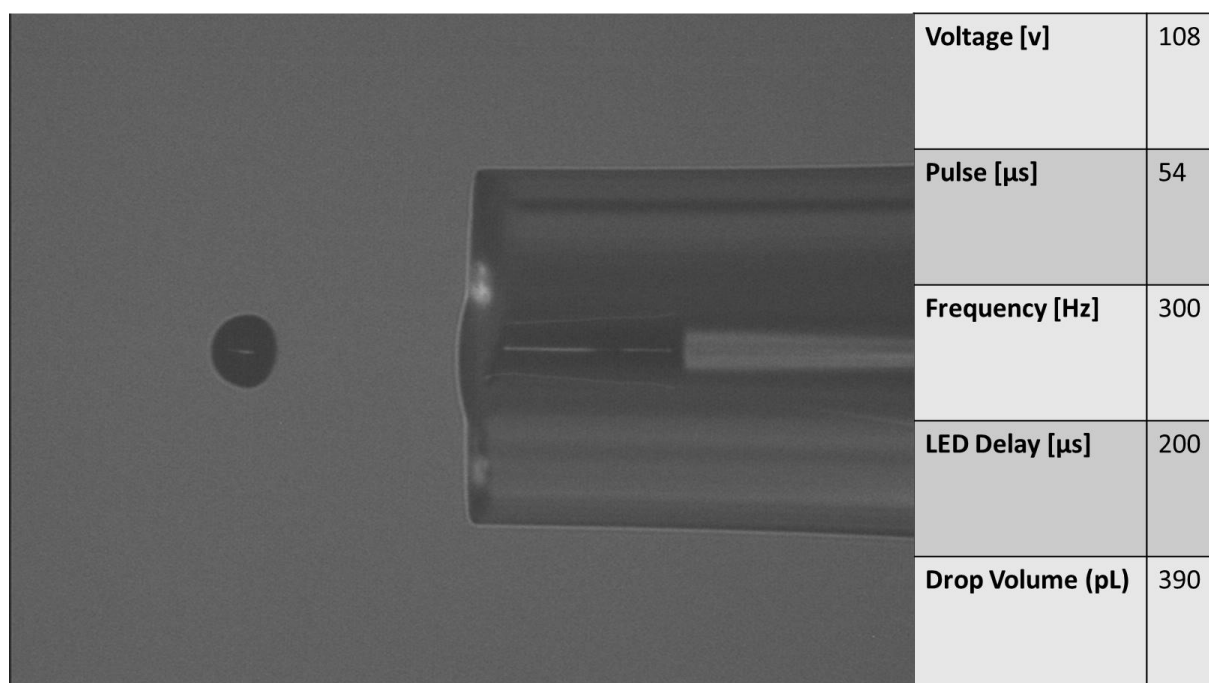
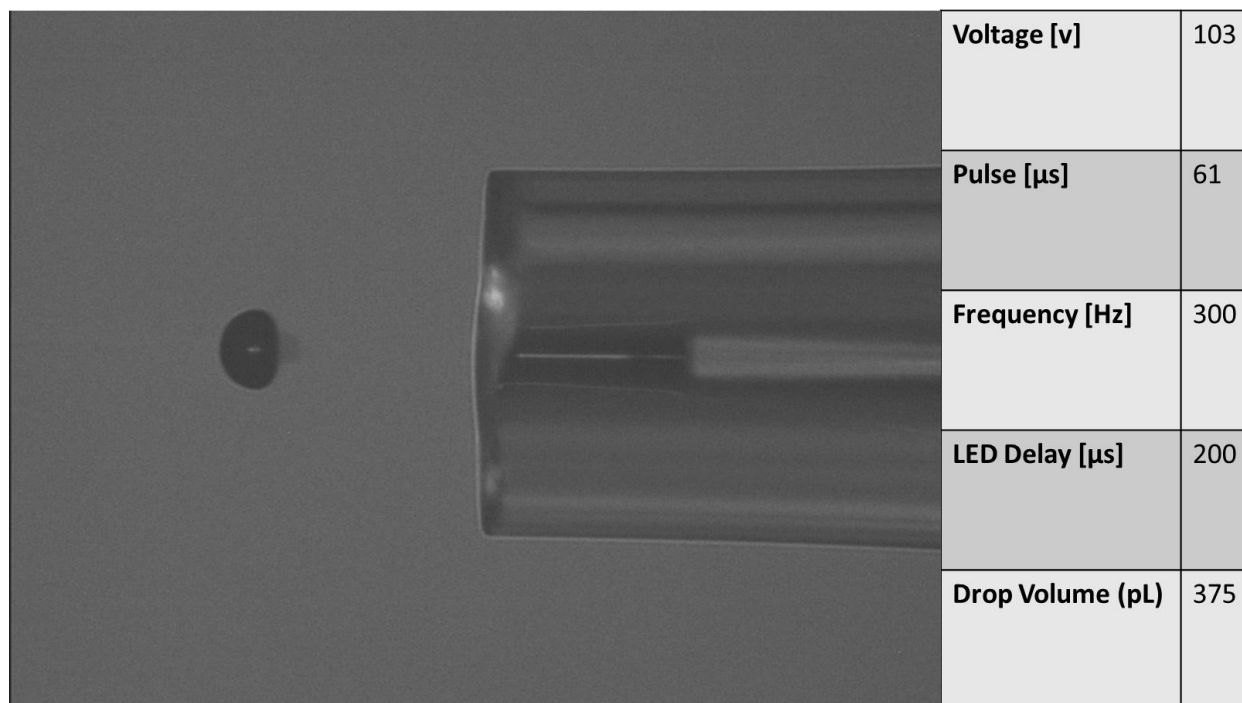


WILEY-VCH

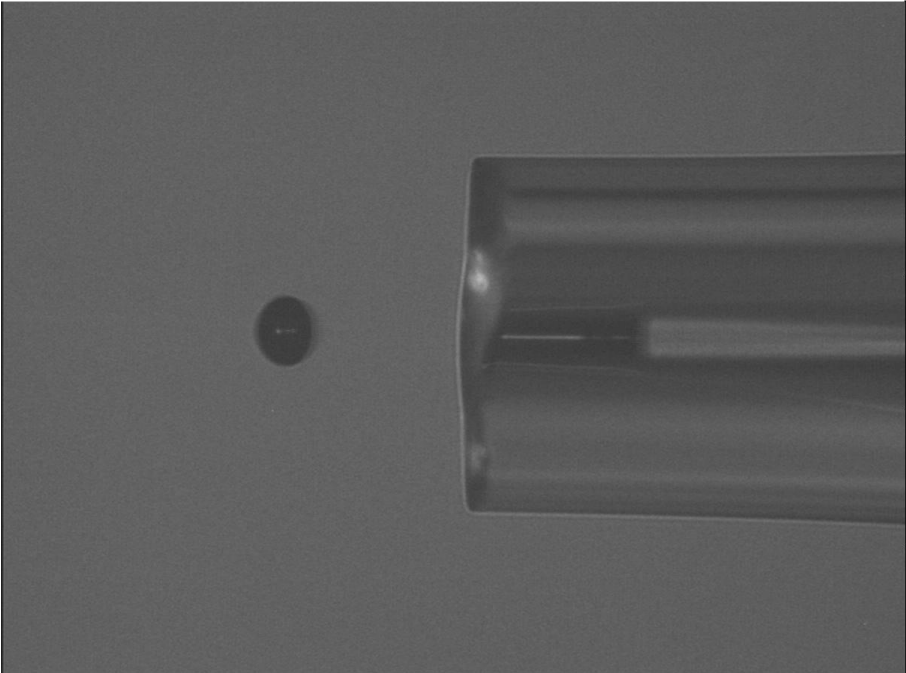


Voltage [v]	106
Pulse [μs]	55
Frequency [Hz]	300
LED Delay [μs]	200
Drop Volume (pL)	394

SI-Figure 2. Droplet formation and printing information for the mPGE-PLGA, PVPVA and mPEG-P ϵ DL printed NPs.



WILEY-VCH

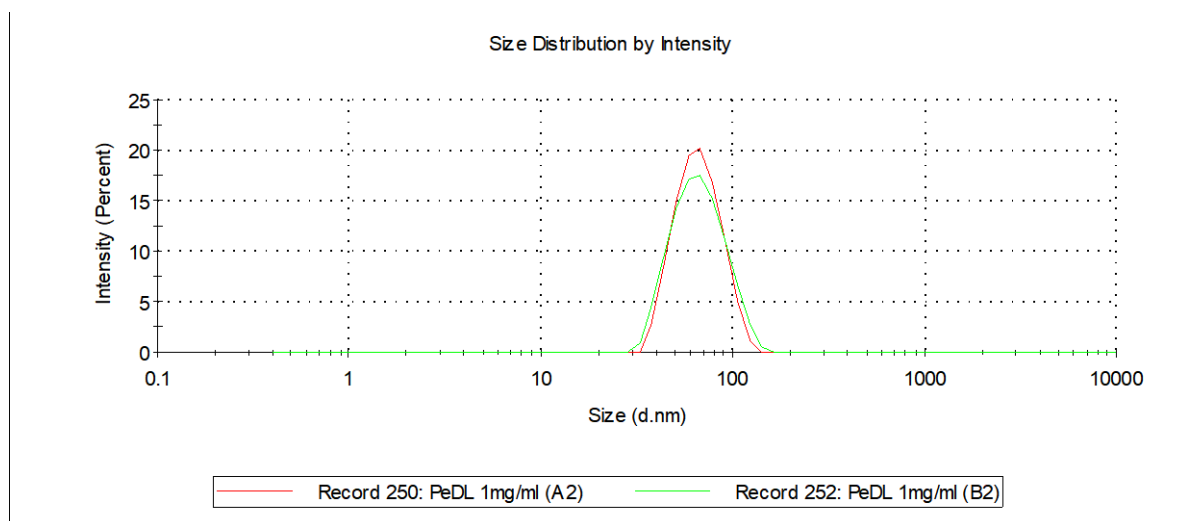


Voltage [v]	100
Pulse [μ s]	54
Frequency [Hz]	300
LED Delay [μ s]	200
Drop Volume (pL)	373

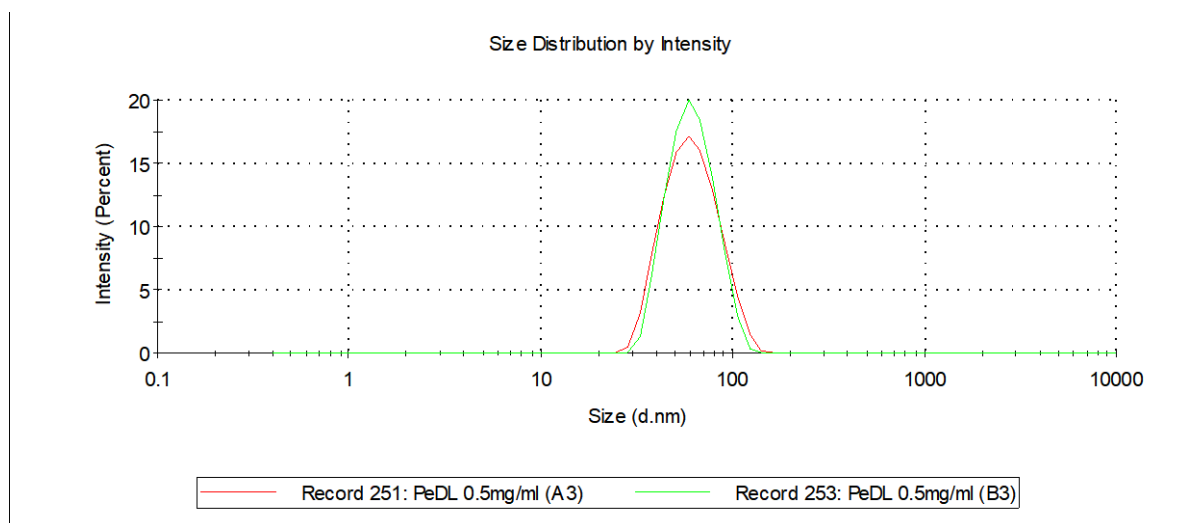
SI-Table 1. Table of the diblock copolymers used, both in the printed and in the "traditional" manual nanoprecipitation method, and resulting NP sizes as measured by dynamic light scattering. Values correspond to averages of 3 measurements.

Polymer	Concentration (mg/mL)	Method	Hydrodynamic Diameter (nm)	Pdi	Figure
mPEG-<i>b</i>-PeDL	1	printed	63.25	0.055	SI-Figure 3
	0.5	printed	57.40	0.086	SI-Figure 4
	2	printed	200.00	0.338	SI-Figure 5 and in SI-Figure 6
mPEG-<i>b</i>-PLGA		manual	154.10	0.221	SI-Figure 6
	1	printed	153.30	0.326	SI-Figure 5 Error! Reference source not found.
	0.5	printed	116.80	0.225	SI-Figure 7 Error! Reference source not found.
mPEG-<i>b</i>-PCL	0.5	printed	366.30	0.393	SI-Figure 7
	0.25	printed	144.80	0.188	

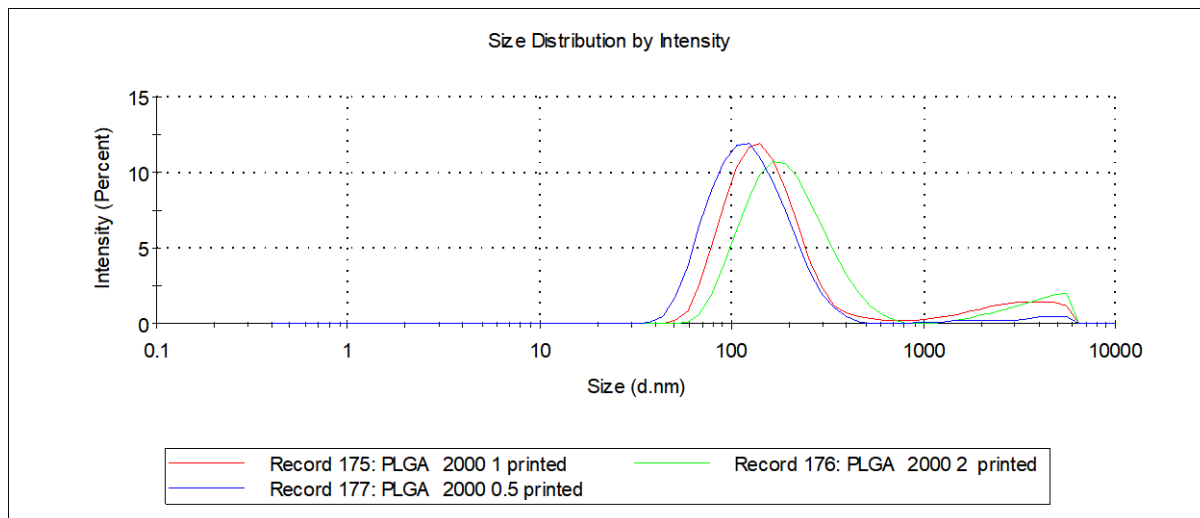
SI-Figure 3. PEG-PeDL NPs prepared in different batches by the printing method show excellent reproducibility.



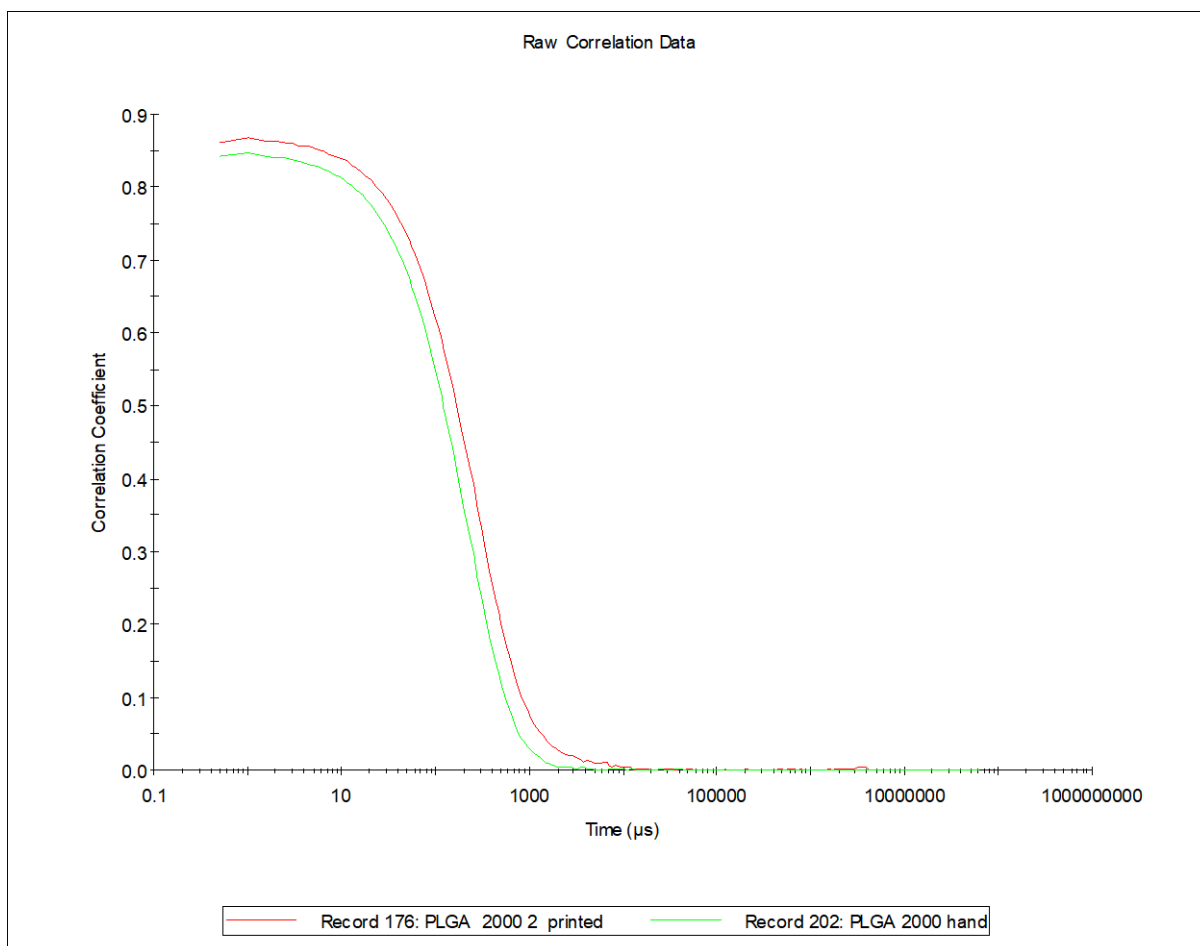
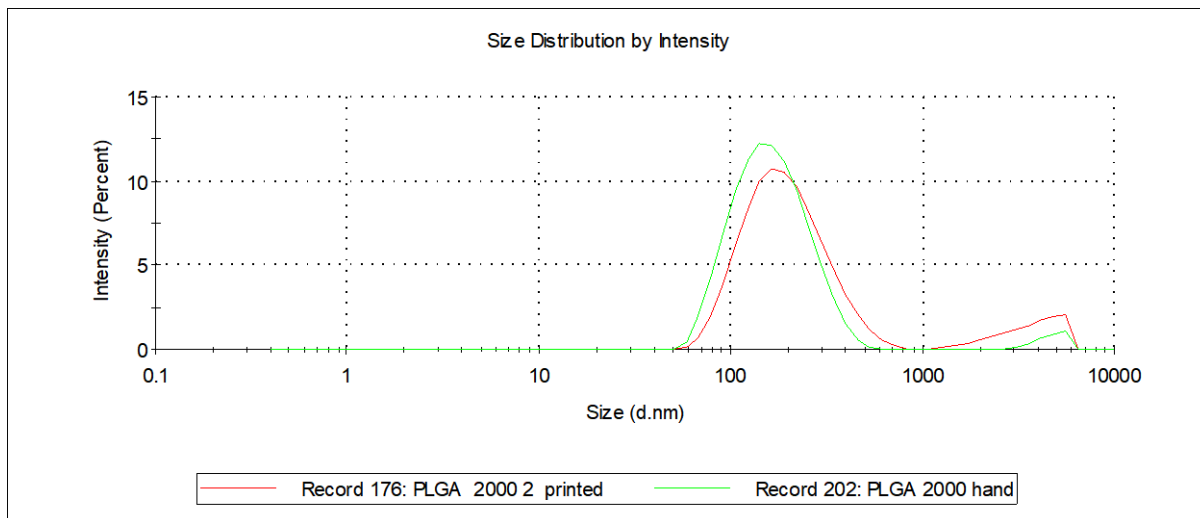
SI-Figure 4. mPEG - PeDL printed NPs in 2 different batches, show excellent reproducibility of the method.



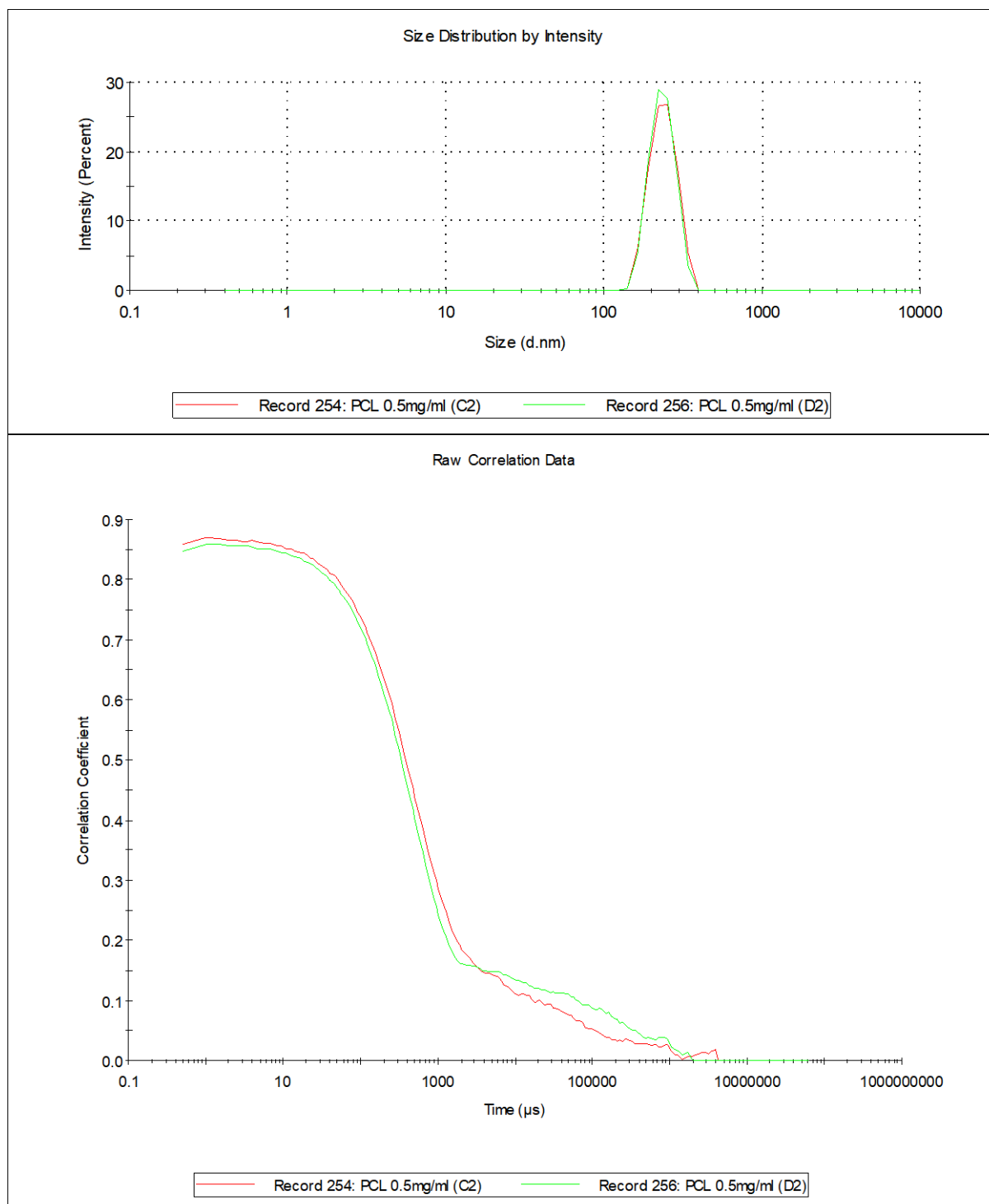
SI-Figure 5. mPEG-PLGA NPs prepared by printing in various concentrations



SI-Figure 6. mPEG-PLGA NPs prepared by printing (red) and manually (green).



SI-Figure 7. mPEG-b-PCL NPs formed at 0.5 mg/mL via the hand method (red line, C2) and via printing (green line, D2). The formation of aggregates is clear from the end shape of the correlogram and the same behaviour is observed visually.



SI-Table 2. Reproducibility of the printing method for two batches on various concentrations.

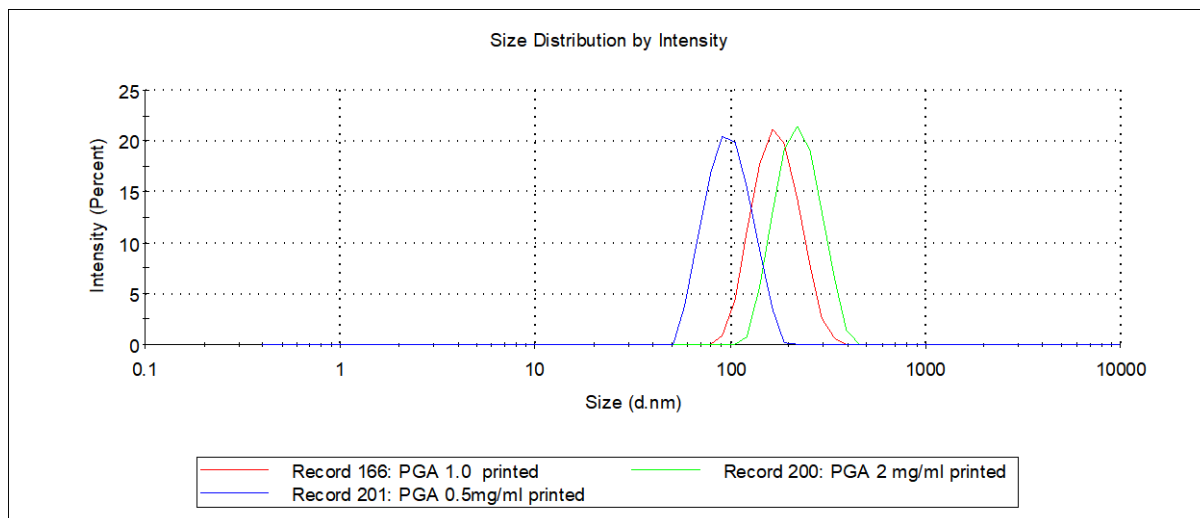
Values correspond to averages of 3 measurements.

Polymer	Concentration (mg/mL)	Method	Hydrodynamic Diameter (nm)	Pdi	Figure
mPEG-<i>b</i>-PeDL	1	printed	63.25	0.055	SI-Figure 3
		printed	62.52	0.090	
	0.5	printed	57.40	0.086	SI-Figure 4
		printed	58.09	0.071	
mPEG-<i>b</i>-PCL	0.5	printed	144.80	0.188	
		printed	280.00	0.37	
PGA	0.5	printed	94.42	0.047	SI-Figure 10
		printed	94.53	0.046	
PGA Trp	1	printed	63.43	0.116	SI-Figure 15
		printed	66.18	0.091	
	0.5	printed	60.94	0.074	SI-Figure 14
		printed	67.83	0.092	
PGA Phe	1	printed	132.30	0.016	SI-Figure 12 Error! Reference source not found.
		printed	134.90	0.017	
	0.5	printed	123.50	0.018	
		printed	123.80	0.021	

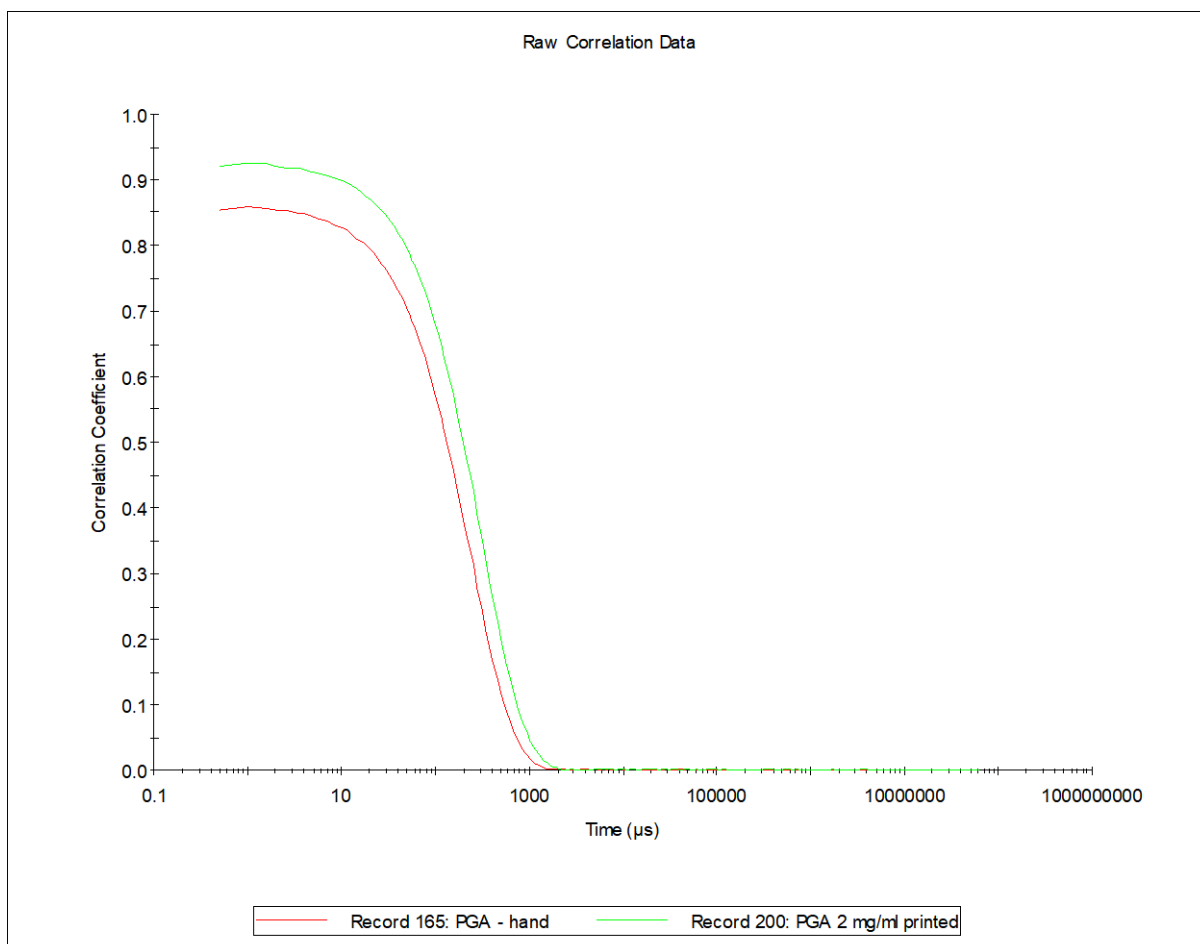
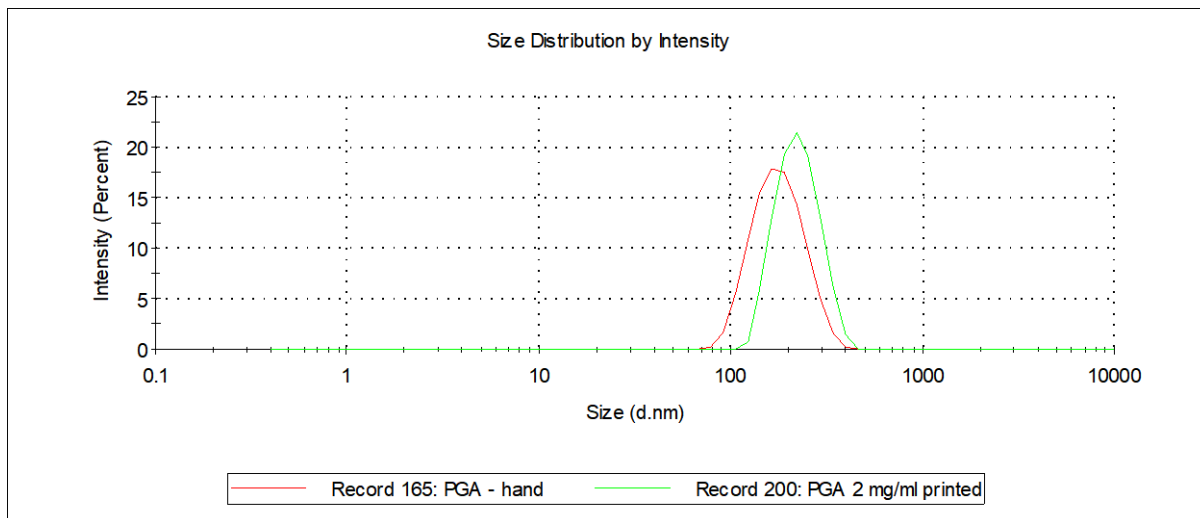
SI_Table 1. Table of the Polyglycerol adipate (PGA) and PGA modified polymers used and resulting NP sizes formed via the printing method, as measured by dynamic light scattering, in comparison with the reported literature values. Values reported via this work (printed) correspond to averages of 3 measurements.

Polymer	Concentration (mg/mL)	Method	Hydrodynamic Diameter (nm)	Pdi	Figure
PGA	2	printed	220.10	0.059	Error! Reference source not found.
		literature	108.45	0.059	-
	0.5	Printed	94.42	0.047	Reference source not found.
		literature	108.00	0.100	-
PGA Phe	0.5	printed	123.50	0.018	Error! Reference source not found.
		literature	108.10	0.015	-
PGA Trp	0.5	printed	60.94	0.074	Error! Reference source not found.
		literature	60.51	0.042	-

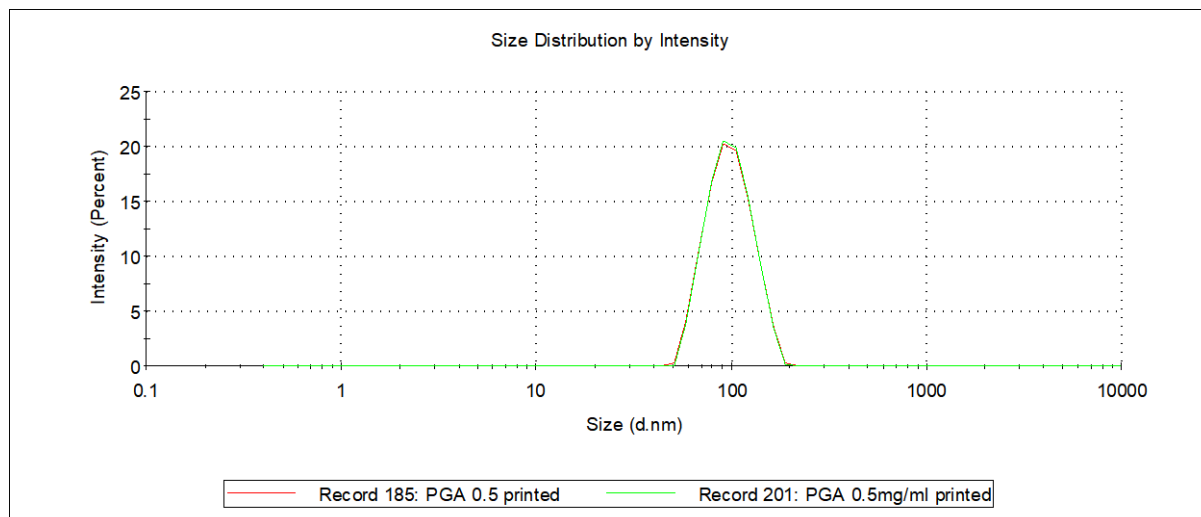
SI-Figure 8. DLS intensity distributions of PGA NPs printed in different concentrations



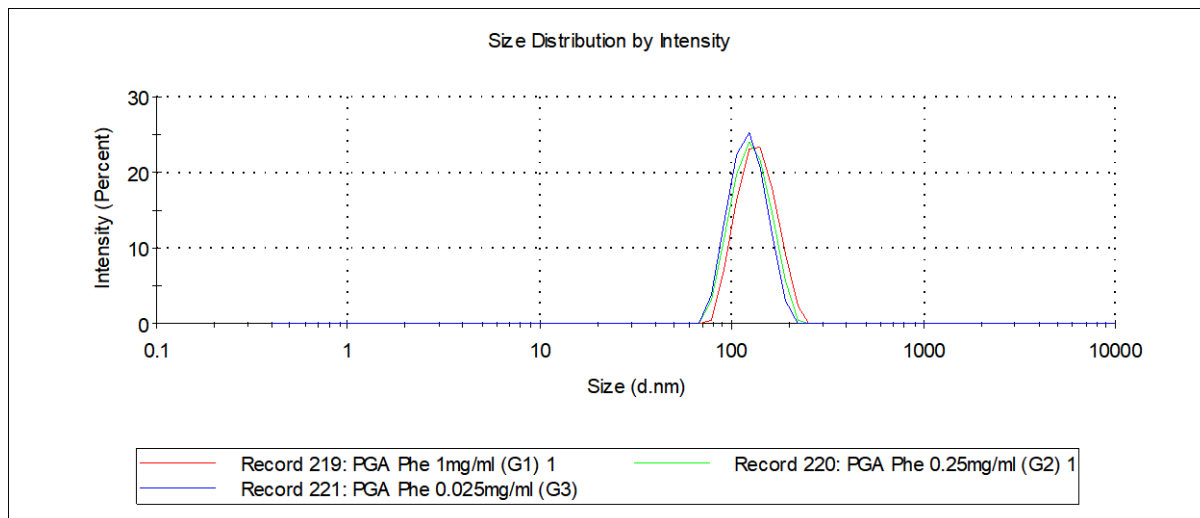
SI-Figure 9. PGA NPs prepared at 2mg/ml manually (red) and via the printing method (green).



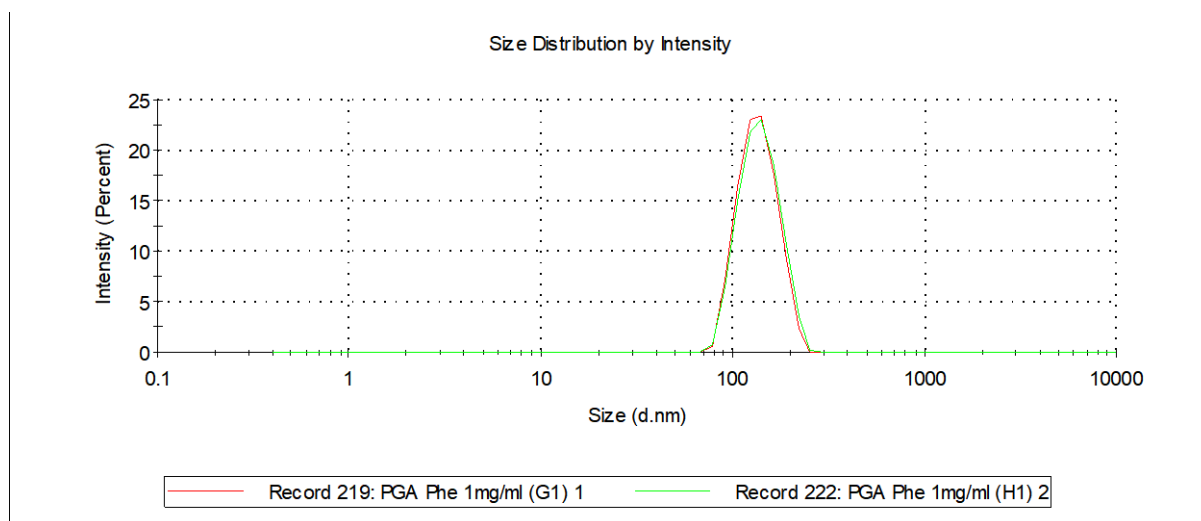
SI-Figure 10. PGA nanoparticles formed by the printing method show batch reproducibility at 0.5 mg/mL.



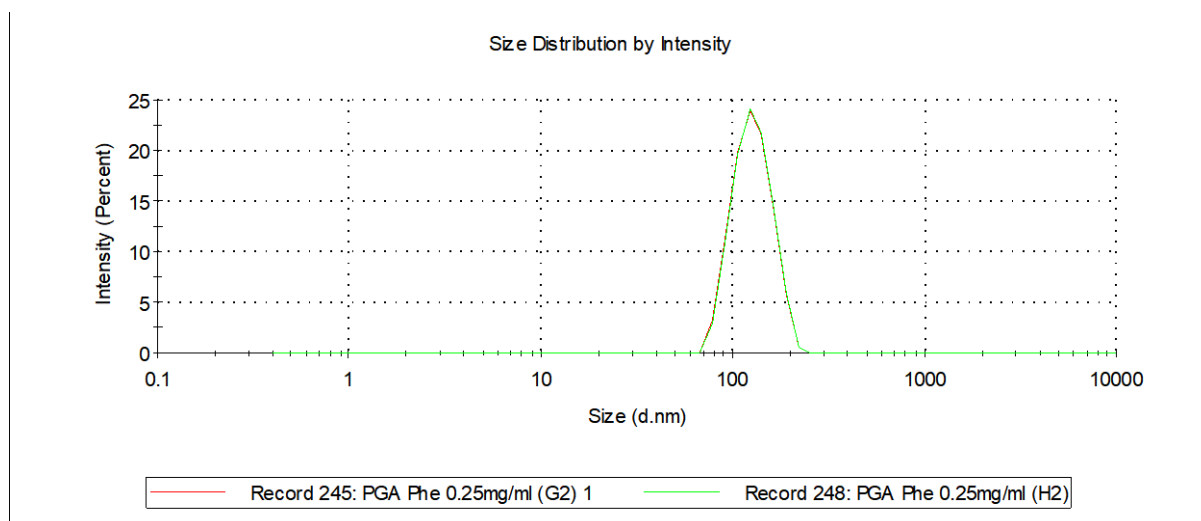
SI-Figure 11. PGA Phenylalanine modified NPs prepared by printing in various concentrations.



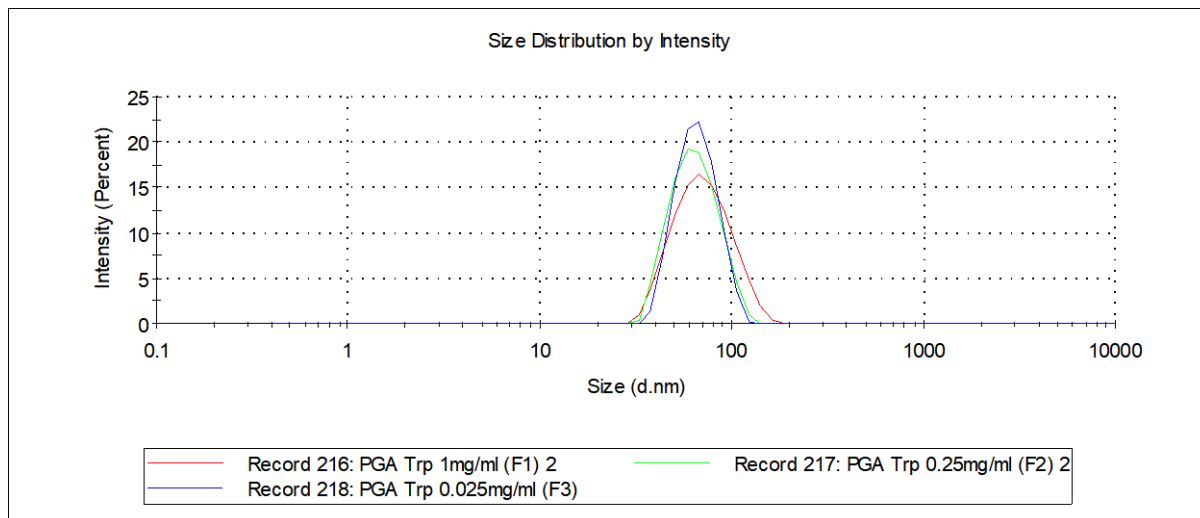
SI-Figure 12. Phenylalanine modified NPs show excellent batch reproducibility by the printing method at 1 mg/mL.



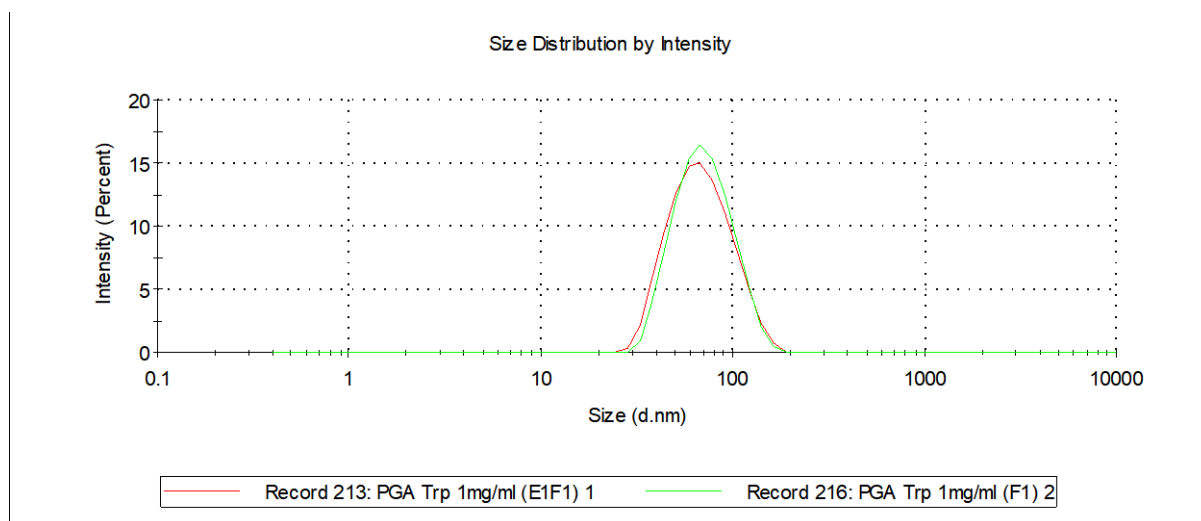
SI-Figure 13. PGA Phenylalanine NPs printed demonstrate excellent batch reproducibility at 0.5 mg/mL (0.25 mg/mL label is wrongly written in the data file).



SI-Figure 14. PGA Tryptophan modified NPs printed at different concentrations.

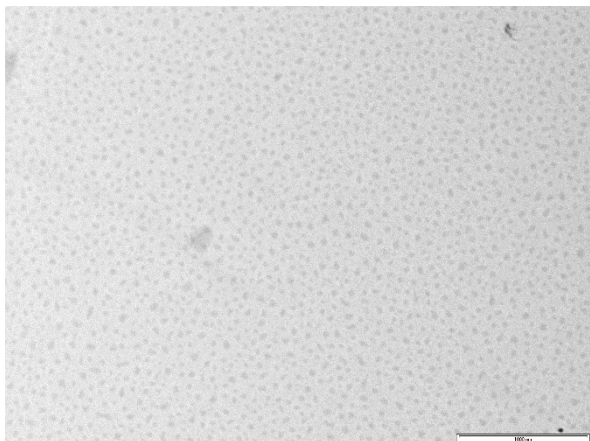


SI-Figure 15. PGA Tryptophan modified NPs show excellent batch reproducibility by the printing method at 1 mg/mL.

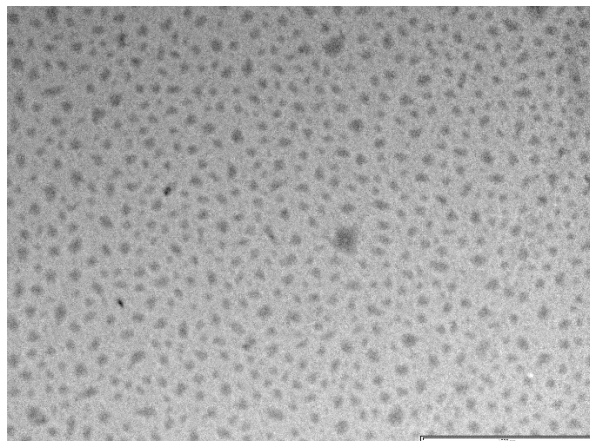


SI-Figure 16 TEM Images of PGA Trp NPs (a) (54 ± 11 nm, $N=100$ particles) and PGA Phe modified (b) (77 ± 18 nm, $N=100$). Scale bar on both is $1\mu\text{m}$.

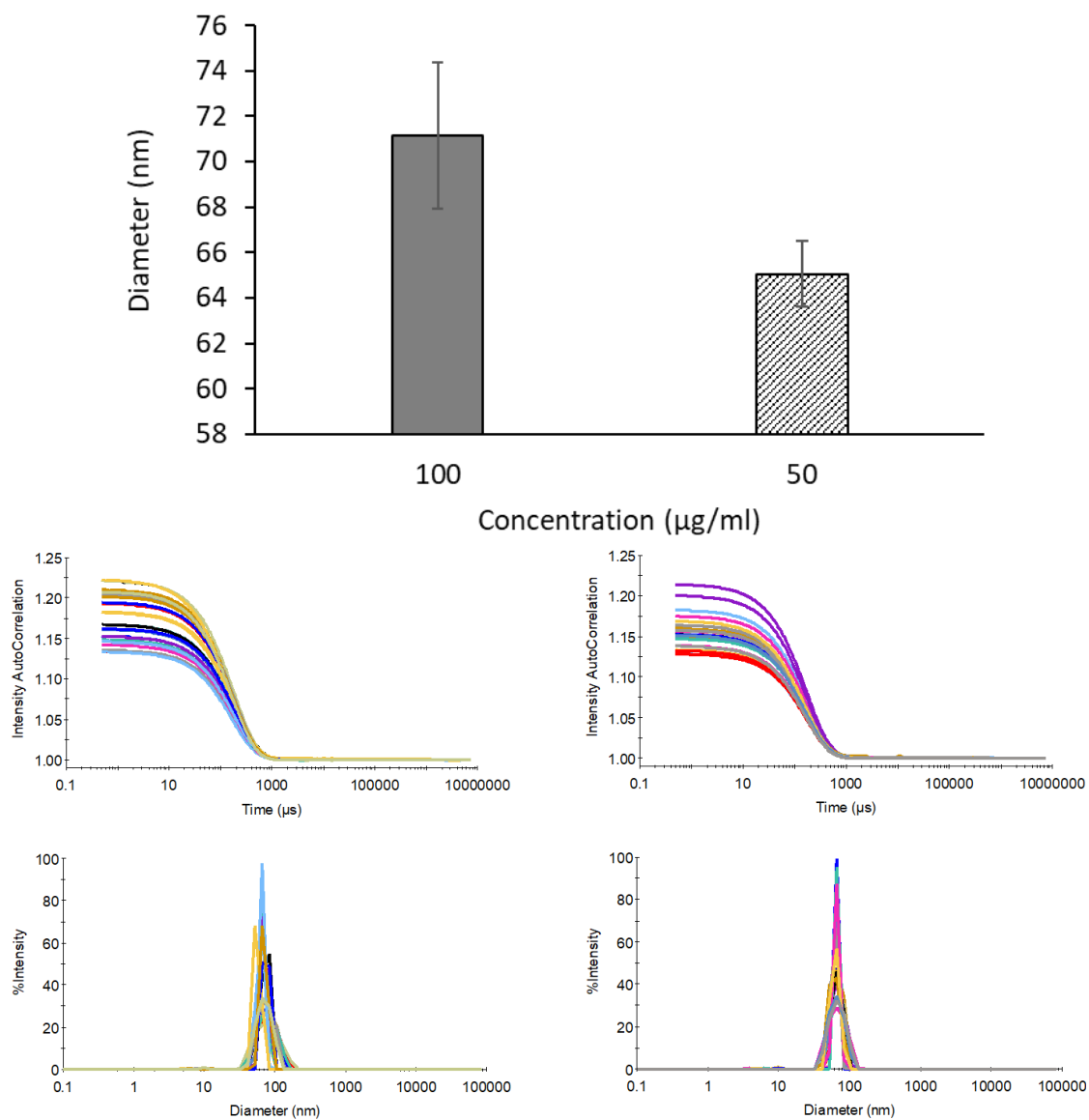
(a)



(b)



SI-Figure 17. Batch correlograms and batch size measurements of PGA nanoparticles, formed in a single printing experiment with 30 replicants for each concentrations, as reported via the High throughput DLS.



SI-Figure 18. Correlograms and size measurements of PGA Tryptophan nanoparticles, formed by printing (left) and via the traditional hand method (right), as reported via the High throughput DLS.

